Resource

Developmental Cell

Compartmentalized localization of perinuclear proteins within germ granules in *C. elegans*

Graphical abstract

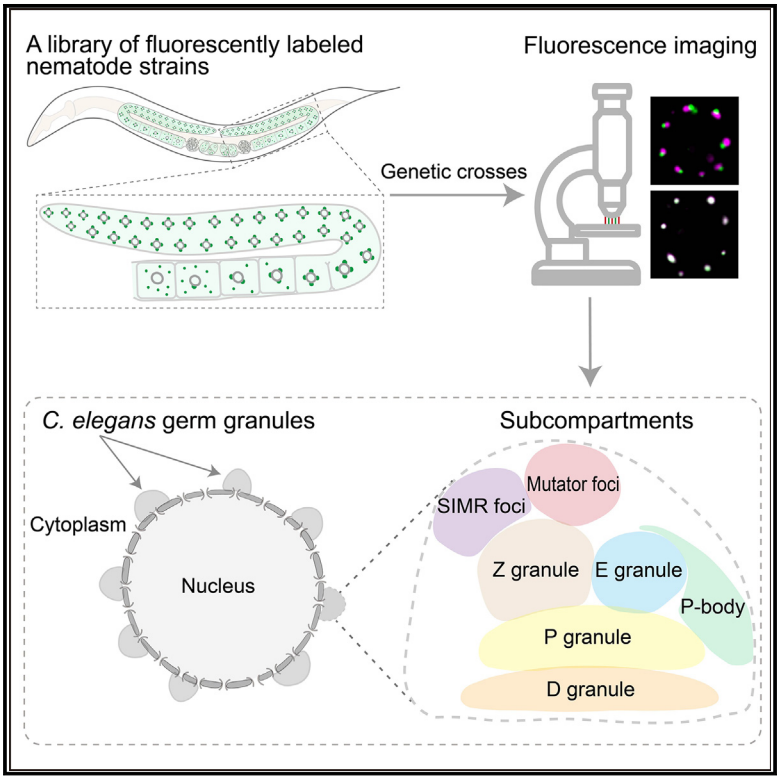

Authors

Xiaona Huang, Xuezhu Feng, Yong-Hong Yan, ..., Xinya Huang, Shouhong Guang, Xiangyang Chen

Correspondence

hxy1996@ustc.edu.cn (X.H.), sguang@ustc.edu.cn (S.G.), xychen91@ustc.edu.cn (X.C.)

In brief

Huang et al. generate a resource of genetically modified nematode strains expressing fluorescently tagged perinuclear proteins. Via fluorescence imaging, they identify the compartmental localization of these proteins in germ granules and advance the characterization of D granules, providing deeper insights into the multiphasic architecture of *C. elegans* germ granules.

Highlights

- Construction of a library of nematode strains expressing fluorescently tagged perinuclear proteins
- The compartmental localization of perinuclear proteins is redefined
- piRNA processing factors are each enriched in particular subcompartments
- D granules are positioned between P granules and nuclear pore complexes

Huang et al., 2025, Developmental Cell *60*, 1–20
April 21, 2025
https://doi.org/10.1016/j.devcel.2024.12.016

CellPress

Please cite this article in press as: Huang et al., Compartmentalized localization of perinuclear proteins within germ granules in *C. elegans*, Developmental Cell (2024), https://doi.org/10.1016/j.devcel.2024.12.016

Developmental Cell

CellPress

Resource

Compartmentalized localization of perinuclear proteins within germ granules in *C. elegans*

Xiaona Huang,[1,4] Xuezhu Feng,[2,4] Yong-Hong Yan,[3,4] Demin Xu,[1] Ke Wang,[1] Chengming Zhu,[1] Meng-Qiu Dong,[3] Xinya Huang,[1,*] Shouhong Guang,[1,5,*] and Xiangyang Chen[1,*]

[1]Department of Obstetrics and Gynecology, The First Affiliated Hospital of USTC, The USTC RNA Institute, Ministry of Education Key Laboratory for Membraneless Organelles & Cellular Dynamics, Hefei National Research Center for Physical Sciences at the Microscale, Center for Advanced Interdisciplinary Science and Biomedicine of IHM, School of Life Sciences, Division of Life Sciences and Medicine, Biomedical Sciences and Health Laboratory of Anhui Province, University of Science and Technology of China, Hefei 230027, China

[2]School of Basic Medical Sciences, Anhui Medical University, Hefei 230032, China

[3]National Institute of Biological Sciences, Beijing 102206, China

[4]These authors contributed equally

[5]Lead contact

*Correspondence: hxy1996@ustc.edu.cn (X.H.), sguang@ustc.edu.cn (S.G.), xychen91@ustc.edu.cn (X.C.)

https://doi.org/10.1016/j.devcel.2024.12.016

SUMMARY

Germ granules, or nuage, are RNA-rich condensates that are often docked on the cytoplasmic surface of germline nuclei. *C. elegans* perinuclear germ granules are composed of multiple subcompartments, including P granules, *Mutator* foci, Z granules, SIMR foci, P -bodies, and E granules. Although many perinuclear proteins have been identified, their precise localization within the subcompartments of the germ granule is still unclear. Here, we systematically labeled perinuclear proteins with fluorescent tags via CRISPR-Cas9 technology. Using this nematode strain library, we identified a series of proteins localized in Z or E granules and extended the characterization of the D granule. Finally, we found that the LOTUS domain protein MIP-1/EGGD-1 regulated the multiphase organization of the germ granule. Overall, our work identified the germ-granule architecture and redefined the compartmental localization of perinuclear proteins. Additionally, the library of genetically modified nematode strains will facilitate research on *C. elegans* germ granules.

INTRODUCTION

Biomolecular condensates are nonmembrane-enclosed organelles that consist of RNAs and proteins, the formation of which is likely elicited by phase separation and mediated by weak and multivalent interactions between RNA, intrinsically disordered proteins, and RNA-binding proteins.[1–3] Common biomolecular condensates include nucleoli, processing (P) bodies, Cajal bodies, stress granules, and germ granules. The molecular constituents within these liquid droplet-like condensates exchange rapidly with the surrounding cellular contents.[4,5] The current model posits that these biomolecular condensates spatiotemporally bring proteins and RNA molecules together to orchestrate complicated RNA processing steps and coordinate gene expression.[4,6]

Many biomolecular condensates contain distinct, immiscible, condensed subcompartments, giving rise to multilayered liquid droplets that may facilitate sequential RNA processing reactions in a variety of RNP bodies.[7–9] For example, the nucleoli usually contain at least three distinct and coexisting subcompartments termed the fibrillar center, dense fibrillar component, and granular component, which are spatially organized, forming layered droplet organization.[8,10] The layered, multiphase droplet nature of nucleoli is thought to facilitate assembly line processing of ribosomal RNA.[8] Recently, high-resolution fluorescence microscopy assays of fluorescent tag-labeled proteins enabled the investigation of the multilayered organization of biomolecular condensates directly in their cellular context and revealed the multiphasic condensate composition and spatial organization of many condensates, such as nucleoli, nuclear speckles, paraspeckles, stress granules, and germ granules.[11–16] Although the underlying molecular mechanisms are largely unknown, the spatial organization of biomolecules into distinct subcompartments within biomolecular condensates may add another layer of internal composition regulation and play a fundamental role in facilitating their complex biological functions.

Germ granules are RNA-rich biomolecular condensates that are often docked at germ cell nuclei.[17–21] Germ granules are widely present in the germ cells of a variety of animals, including worms, flies, zebrafish, Xenopus, and mice.[21–26] Recent studies have suggested that *C. elegans* germ granules are subcompartmentalized into several distinct regions that enclose particular sets of proteins, including P granules, *Mutator* foci, Z granules, SIMR foci, P-bodies, and E granules.[21,27,28] The P granule exhibits multiple liquid-like behaviors and has emerged as a

Please cite this article in press as: Huang et al., Compartmentalized localization of perinuclear proteins within germ granules in *C. elegans*, Developmental Cell (2024), https://doi.org/10.1016/j.devcel.2024.12.016

leading model for the study of biomolecular condensates.[29,30] PGL-1 is a germline-expressed protein that is widely used as a marker protein of P granules.[31] The Z granule contains ZNFX-1 and WAGO-4, which promote RNAi inheritance.[14,32,33] The *Mutator* foci and E granule are two independent germ granule compartments required for 22G RNA generation using a largely nonoverlapping set of RNA transcripts as templates.[28,34,35] SIMR foci, which are marked by SIMR-1, promote small interfering RNA (siRNA) amplification from piRNA targets and drive small RNA specificity for the nuclear Argonaute protein HRDE-1.[36,37] P-bodies, which are marked by CGH-1, are cellular aggregates of translationally repressed mRNPs that usually degrade mRNAs and inhibit their translation.[27,38,39] Remarkably, these immiscible germ-granule compartments are not randomly ordered with respect to each other. For example, many germ granules contain a single Z granule sandwiched between a P granule and a *Mutator* focus, forming ordered tri-condensate assemblages termed PZM granules.[14] However, little is known about how and why *C. elegans* germ granules are divided into so many granular subcompartments and whether uncharted germ-granule compartments await discovery.

The multiphasic *C. elegans* germ granule provides multiple unique subcompartments to organize perinuclear proteins and establish highly sophisticated perinuclear gene regulation networks, including small RNA-based gene regulatory pathways.[21,23,40] For instance, many *Mutator* factors accumulate at *Mutator* foci, contributing to siRNA amplification from poly(UG)-tailed RNA templates to promote gene silencing.[35,41,42] However, the biological functions of most germ-granule compartments are largely unknown. For example, although ZNFX-1, WAGO-4, and LOTR-1 localize in Z granules, both ZNFX-1 and WAGO-4 promote RNAi inheritance, whereas *lotr-1* mutants display enhanced RNAi inheritance, suggesting that the Z granule may play multiple roles in the inheritance of RNAi.[14,32,43] Determining the compartmental localization of perinuclear proteins or the proteomes of specific germ-granule compartments may help comprehensively understand the cellular functions of each germ-granule compartment. For instance, the identification of SIMR foci-localized proteins improves our understanding of the biological functions of SIMR foci, such as siRNA amplification from piRNA targets and the driving of small RNA specificity for Argonaute proteins.[36,37] Approximately 90 *C. elegans* proteins have been found to be enriched in the germ granule.[21,28,37,44,45] Yet, the precise localization of many of these proteins within the germ granule is still unclear. Deciphering the suborganelle localization of perinuclear proteins may help comprehensively understand the biological functions of each germ-granule compartment in perinuclear RNA processing and gene regulation networks.

Here, we systematically labeled reported perinuclear proteins with fluorescent tags via CRISPR-Cas9 technology. We re-explored the perinuclear localization of these proteins and corrected some ambiguous and missing annotations in previous studies. We found that proteins participating in distinct piRNA processing steps were each enriched in particular germ-granule compartments. We extended the characterization of the D granule that localized between the P granule and the nuclear pore complex (NPC). Furthermore, we found that the architecture of the germ granule was maintained by the LOTUS domain protein MIP-1/EGGD-1. Overall, our work revealed the architecture of the multilayered germ granule and provided a resource for investigating perinuclear proteins in *C. elegans*.

RESULTS

Systematic labeling of perinuclear proteins with fluorescent tags via CRISPR-Cas9 technology

The current model posits that *C. elegans* germ granules are divided into at least 6 subcompartments, including P granules, *Mutator* foci, Z granules, SIMR foci, P-bodies, and E granules (Figure 1A).[21,27,28] These subcompartments, in which distinct sets of proteins have been identified, are assembled in an orderly manner outside the nuclear envelope.[21] Additionally, we revealed that DDX-19 was enriched in a distinct subcompartment, termed the D granule in this study (Figure 1A). Particular proteins were used as marker proteins to visualize each subcompartment (Figure 1B).[14,27,28,35,36,38,46,47,49]

More than half of the perinuclear proteins were previously annotated to be enriched in the P granule.[21] However, improvements in microscopy resolution and the identification of more subcompartments prompted us to reinvestigate the localization of the reported perinuclear proteins within germ granules. Thus, we systematically tagged these proteins with fluorescent tags via CRISPR-Cas9 technology (Figures 1C, S1A, and S1B). In this study, we successfully tagged 44 proteins with fluorescent tags. These insertions were confirmed via both genotyping and fluorescence analysis (Figures 1D and S1B). As most of these genes are required for fertility,[21] we assessed the brood size of these strains and did not find significant alterations in most of the strains compared with N2 (wild-type) worms (Figures S1C and S1D), suggesting that the fluorescence-tagged proteins largely recapitulated their endogenous functions. We further collected nematode strains expressing fluorescence-tagged perinuclear proteins, which were constructed previously in our laboratory.[28,50–52] In total, we collected a nematode strain library that consists of 80 strains covering 65 genes (Table S1).

We further examined whether the same proteins with different tags colocalized with each other. We crossed animals expressing the same proteins labeled with different fluorescent tags and examined their localization in F1 heterozygous animals, such as PGL-1, ZNFX-1, CSR-1, and DEPS-1 (Figure 1E). The results suggested that labeling of perinuclear proteins with different fluorescent tags did not obviously affect their perinuclear condensation or localization (Figure 1E).

Systematic investigation of the compartmental localization of perinuclear proteins within the germ granule

On the basis of the strain library, we then systematically examined the perinuclear localization of these proteins within the germ granule via fluorescence imaging. Notably, although most of these proteins were expressed throughout the germline during development, we only imaged these proteins in the pachytene cells of day 1 self-fertile adult hermaphrodites in this study. Moreover, most of these proteins localize to both the cytosol and germ granules in germ cells, especially P-body

Please cite this article in press as: Huang et al., Compartmentalized localization of perinuclear proteins within germ granules in *C. elegans*, Developmental Cell (2024), https://doi.org/10.1016/j.devcel.2024.12.016

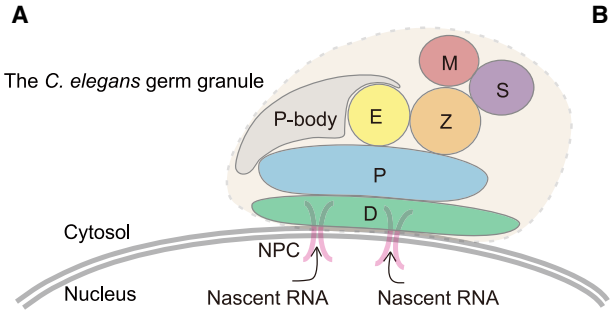

B

Subcompartments of the germ granule	Marker	References
D (D granule)	DDX-19	This study and ref [46]
P (P granule)	PGL-1	refs [14, 49]
Z (Z granule)	ZNFX-1	ref [14]
M (Mutator foci)	MUT-16	ref [35]
S (SIMR foci)	SIMR-1	ref [36]
E (E granule)	ELLI-1	refs [28, 47]
P-body	CGH-1	refs [27, 38]

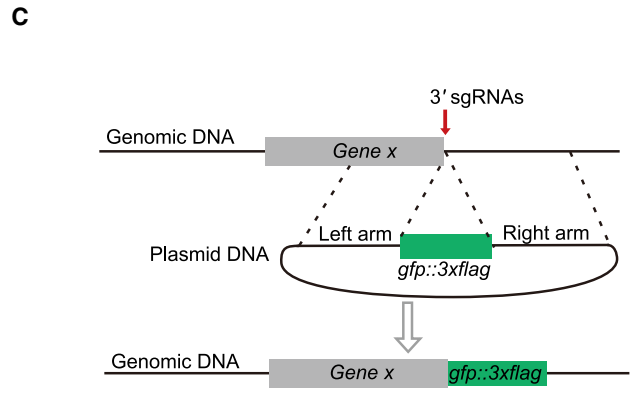

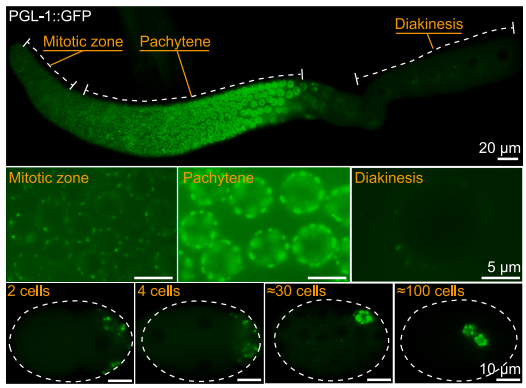

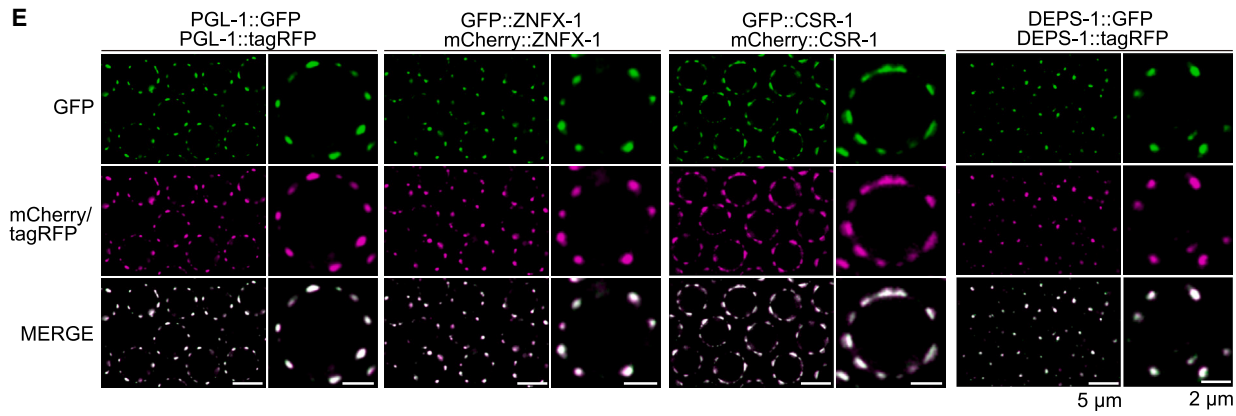

Figure 1. Systematic labeling of perinuclear proteins with fluorescent tags via CRISPR-Cas9 technology

(A) Model of germ-granule architecture in *C. elegans* pachytene cells. Note that the relative positions of different germ-granule compartments in this model were inferred from imaging of multiple sets of two or three condensates.[14,27,28,36,46,47] Moreover, compositional condensates vary mildly among different perinuclear germ granules, and the shapes of particular germ-granule compartments may also be dynamic, for example, the toroid shape of a subset of P granules in late pachytene cells.[48] Therefore, this model only indicates that at least seven subcompartments act as optional units in germ-granule assembly in pachytene cells and roughly shows the shapes and spatial organization of different germ-granule compartments. The precise spatial organization of each subcompartment within germ granules is still largely unknown.

(B) Summary of the marker proteins of each germ-granule compartment.

(C) Schematic of the insertion of DNA elements encoding GFP::3xFLAG into designed genomic loci via CRISPR-Cas9 technology.

(D) Fluorescence micrographs of the germline and embryos dissected from adults expressing PGL-1::GFP.

(E) Fluorescence micrographs of pachytene germ cells that express the indicated fluorescent proteins.

See also Figures S1 and S2 and Table S1.

Please cite this article in press as: Huang et al., Compartmentalized localization of perinuclear proteins within germ granules in *C. elegans*, Developmental Cell (2024), https://doi.org/10.1016/j.devcel.2024.12.016

Table 1. Summary of the compartmental localization of perinuclear proteins in germ granules of pachytene cells

Localization	Protein	Human ortholog (Wormbase)	Figure/Ref	Domain/cellular function (Phillips and Updike[21] and Wormbase)
P granule	PGL-1	–	Kawasaki et al.[49]	RNA endoribonuclease
	FBF-2	–	Figure S2A	Pumilio-family RNA-binding domain
	GLD-1	QKI (QKI, KH domain-containing RNA binding)	Figure S2A	RNA-binding KH domain
	GLD-2	TENT2 (terminal nucleotidyltransferase 2)	Figure S2A	Poly(A) polymerase
	GLD-3	–	Figure S2A	KH RNA-binding domain
	GLH-1	DDX4 (DEAD-box helicase 4)	Figure 2A	Vasa DEAD-box helicase
	GLH-2	DDX4 (DEAD-box helicase 4)	Figure S2B	Vasa DEAD-box helicase
	GLS-1	–	Figure S2A	germ cell fate decision
	HENN-1	HENMT1 (HEN methyltransferase 1)	Figure 3J	2′-O-methyltransferase
	IFE-1	EIF4E and EIF4E1B (eukaryotic translation initiation factor 4E family)	Figure S2A	mRNA cap-binding
	LAF-1	DDX3X (DEAD-box helicase 3 X-linked) and DDX3Y (DEAD-box helicase 3 Y-linked)	Figure S2A	DEAD-box helicase
	PGL-2	–	Figure 2A	PGL family protein of unknown function
	PGL-3	–	Figure 2A	RNA endoribonuclease and P granule assembly
	PUF-8	PUM1 and PUM2 (pumilio RNA-binding family member 1 and 2)	Figure S2A	Pumilio-family RNA-binding domain
	RDE-12	Probable ATP-dependent RNA helicase DDX4	Figure S2A	DEAD-box helicase
	RNP-8	–	Figure S2A	RRM RNA-binding domain
	VBH-1	DDX3X (DEAD-box helicase 3 X-linked)	Figure S2A	Vasa- and Belle-like DEAD-box helicase
	WAGO-1	–	Figure 2A	Argonaute binding to 22G RNAs
Z granule	ZNFX-1	ZNFX1 (zinc finger NFX1-type containing 1)	Wan et al.[14]	NFX1-type zinc finger domain
	DEPS-1	–	Figure 2B	P granule assembly and piRNA-based silencing
	GLH-3 [a]	DDX4 (DEAD-box helicase 4)	Figure 2D	Vasa DEAD-box helicase
	GLH-4	–	Figure 2D	Vasa DEAD-box helicase
	LOTR-1	–	Figure S2A	LOTUS and Tudor domains
	MIP-2/EGGD-2	–	Figure 2D	LOTUS domain
	PARN-1	PNLDC1 (PARN like ribonuclease domain-containing exonuclease 1)	Figure 3F	piRNA 3′–5′ exoribonuclease
	PID-4	–	Figure S4H and S4I	piRNA-induced gene silencing
	PID-5	XPNPEP1 (X-prolyl aminopeptidase 1)	Figure S4J and S4K	piRNA-induced gene silencing
	PRG-1[a]	PIWIL1 and PIWIL3 (piwi like RNA-mediated gene silencing 1 and 3)	Figure 3F	PIWI protein binding to 21U RNAs (piRNAs)
Mutator foci	MUT-16	–	Phillips et al.[35]	*Mutator* foci formation and siRNA amplification
	MUT-2	–	Figure S2A	poly(UG) polymerase
	RRF-1	–	Chen et al.[28] and Phillips et al.[35]	RNA-directed RNA polymerase (RdRP)
SIMR foci	SIMR-1	–	Manage et al.[36]	siRNA defective Tudor-domain protein
	HRDE-2	–	Figure S2A and Chen and Phillips[37]	HELICc domain

(*Continued on next page*)

Please cite this article in press as: Huang et al., Compartmentalized localization of perinuclear proteins within germ granules in *C. elegans*, Developmental Cell (2024), https://doi.org/10.1016/j.devcel.2024.12.016

Table 1. ***Continued***

Localization	Protein	Human ortholog (Wormbase)	Figure/Ref	Domain/cellular function (Phillips and Updike[21] and Wormbase)
P-body	CGH-1	DDX6 (DEAD-box helicase 6)	Du et al.[27]	Dhh1/DDX6 DEAD-box helicase
	CAR-1	LSM14B (LSM family member 14B)	Figure S2D	cytokinesis, apoptosis, and RNA-associated
	EDC-3	EDC3 (enhancer of mRNA decapping 3)	Zhang et al.[52]	enhancer of mRNA decapping
	IFE-3	EIF4E and EIF4E1B (eukaryotic translation initiation factor 4E family)	Figure S4E	mRNA cap-binding
	IFET-1	EIF4ENIF1 (eukaryotic translation initiation factor 4E nuclear import factor 1)	Figure S2D	eIF4E transporter
	NHL-2	TRIM45 (tripartite motif containing 45)	Figure S2D	DEAD/H-box RNA helicase binding activity
E granule	ELLI-1	–	Chen et al.[28]	E granule assembly and siRNA biogenesis
	DRH-3 [a]	RIGI (RNA sensor RIG-I)	Chen et al.[28]	Dicer-related DEAD-box helicase
	EGC-1	–	Chen et al.[28]	E granule assembly
	EGO-1[a]	–	Chen et al.[28]	RNA-directed RNA polymerase (RdRP)
	EKL-1[a]	–	Chen et al.[28]	siRNA biogenesis
	ERH-2	ERH (ERH mRNA splicing and mitosis factor)	Figure 3C	piRNA biogenesis and cell division
	PICS-1/PID-3	–	Figure 3C	piRNA biogenesis and cell division
	PID-1	–	Figure 3C	piRNA biogenesis
	TOFU-6	–	Figure 3C	piRNA biogenesis and cell division
D granule	DDX-19	DDX19A and DDX19B (DEAD-box helicase 19A and 19B)	Figure 4B and Sheth et al.[46]	DEAD-box helicase
	CSR-1[a]	–	Figure 4F and 4G	Essential Argonaute binding to 22G RNAs
NPCs	NXF-1	NXF1; NXF2 and NXF2B (nuclear RNA export factor)	Figure S5I	NXF1/TAP-like mRNA export factor
	NPP-9	RANBP2 (RAN binding protein 2)	Figure 4A	nuclear pore complex protein
Unknown	PLP-1	PURB (purine rich element binding protein B)	Figure S2E	Pur alpha-like protein
	PAB-1	PABPC1; PABPC3 and PABPC4 (poly(A) binding protein)	Figure S2E	poly(A)-binding protein
	MINA-1	–	Figure S2E	mRNA binding and inhibitor of apoptosis
	DCAP-1	DCP1A and DCP1B (decapping mRNA 1A and 1B)	Figure S2D	mRNA decapping enzyme
	GLD-4	TENT4A and TENT4B (terminal nucleotidyltransferase 4A and 4B)	Figure S2E	poly(A) polymerase

[a]GLH-3, PRG-1, and CSR-1 partially localized to P granules; EGO-1, DRH-3, and EKL-1 partially localized to Mutator foci.

proteins, yet we have focused mainly on deciphering their localization within germ granules.

To examine whether these perinuclear proteins were enriched in particular subcompartments of the germ granule reported in the literature, we crossed these fluorescent proteins into animals expressing corresponding marker proteins and imaged the animals. The localization of most of these proteins was consistent with the literature[21,37,53] (Figures S2A–S2D). Several proteins, such as DCAP-1, MINA-1, PAB-1, PLP-1, and GLD-4, presented poor perinuclear accumulation, making it difficult to clarify their intragranular positioning (Figures S2D and S2E). However, a considerable number of proteins, which were previously considered P granule components, accumulated in other subcompartments of the germ granule. For proteins whose compartmental localization differed from that reported in the literature, on the basis of shapes and sizes of their perinuclear foci in pachytene cells and the dynamic formation of their foci during development,[14,28,54] we first empirically assessed the subcompartments in which these proteins may accumulate. We then crossed these tagged proteins with the corresponding marker strains to confirm their colocalization. Lastly, their compartmental localization was further verified by examining their localization in mutants with defects in the perinuclear assembly of particular germ-granule compartments, for example, in *pid-2(-)* and *mip-1(-)* animals.[15,44,45,55,56] The compartmental localization of perinuclear proteins revealed by the above strategy is summarized in Table 1. Notably, labeling perinuclear proteins with different fluorescent tags may affect their localization/condensation under stress conditions, as it has been reported that labeling PGL-1 with different fluorescent tags affects its condensation upon stress treatment.[57]

Please cite this article in press as: Huang et al., Compartmentalized localization of perinuclear proteins within germ granules in *C. elegans*, Developmental Cell (2024), https://doi.org/10.1016/j.devcel.2024.12.016

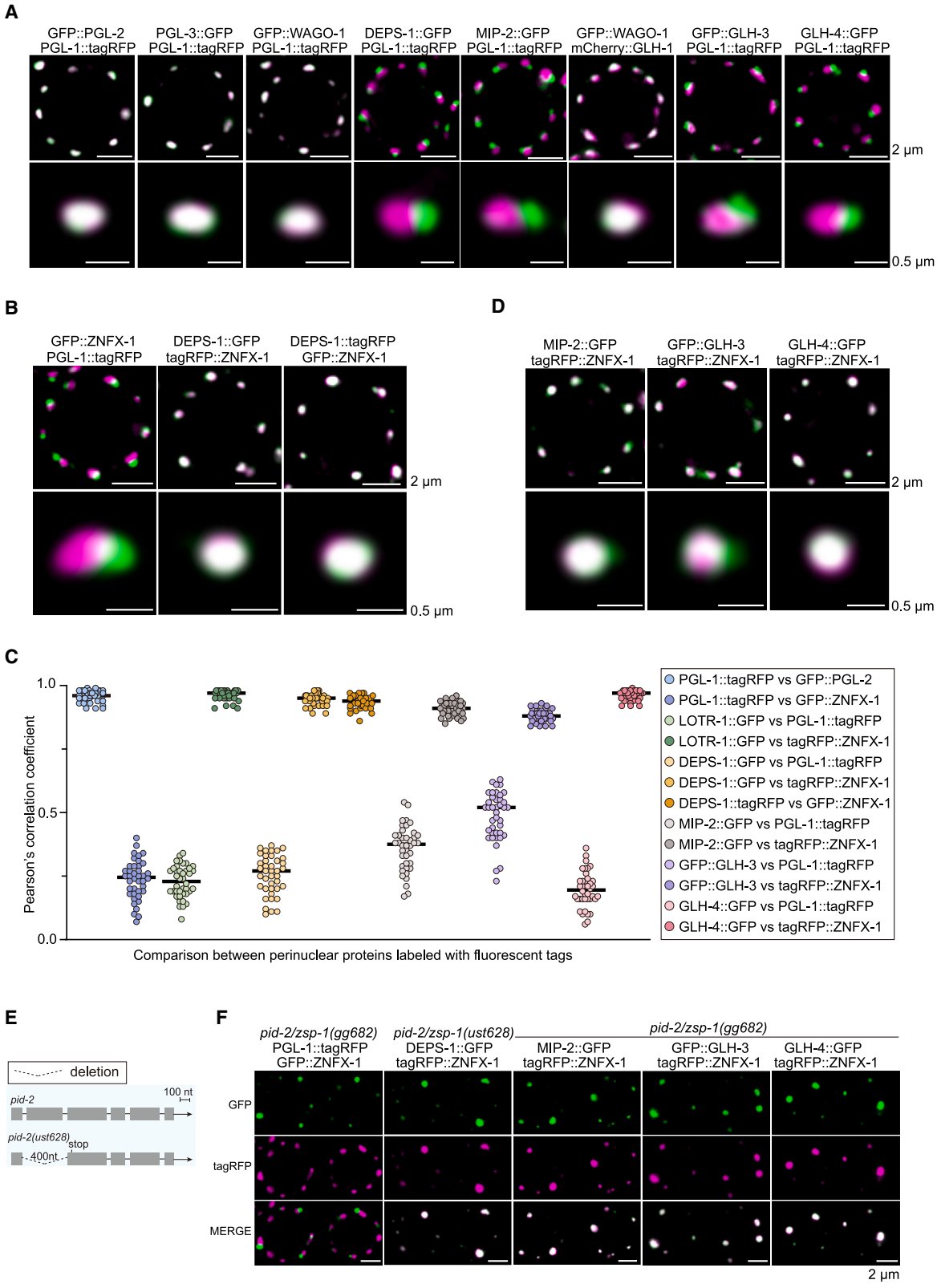

(legend on next page)

Please cite this article in press as: Huang et al., Compartmentalized localization of perinuclear proteins within germ granules in *C. elegans*, Developmental Cell (2024), https://doi.org/10.1016/j.devcel.2024.12.016

DEPS-1, MIP-2, GLH-3, and GLH-4 were enriched in Z granules

We first examined the localization of common P granule markers and the factors required for P granule assembly. PGL-1::tagRFP was used as the marker of P granules.[14,49] PGL family proteins, including PGL-1, PGL-2, and PGL-3, localize to perinuclear condensates and function redundantly in *C. elegans* germline development.[58] As reported previously, GFP::PGL-2 and PGL-3::GFP colocalized with PGL-1::tagRFP in the P granule (Figure 2A). WAGO-1, an Argonaute protein involved in the RNAi pathway, also colocalized with PGL-1::tagRFP, as previously reported (Figure 2A).[60]

DEPS-1, which interacts with PRG-1, ZNFX-1, and LOTR-1 in germ cells, promotes piRNA-dependent silencing and RNAi inheritance.[43,61,62] DEPS-1 also promotes P granule assembly, germ cell proliferation, and fertility.[61,63] Unexpectedly, DEPS-1::GFP did not colocalize with PGL-1::tagRFP but colocalized with tagRFP::ZNFX-1 (Figures 2A and 2B). Similarly, DEPS-1::tagRFP colocalized with GFP::ZNFX-1 (Figure 2B). Image quantification of the spatial overlap between these fluorescence signals further revealed that DEPS-1 was a Z granule component (Figure 2C). These results also suggested that labeling DEPS-1 with different fluorescent tags did not affect its accumulation in Z granules.

MIP-1/EGGD-1 and MIP-2/EGGD-2 are two LOTUS domain-containing proteins that recruit *C. elegans* Vasa to perinuclear germ granules.[44,45] Animals lacking MIP-1/EGGD-1 and MIP-2/EGGD-2 exhibit P granule detachment from the nuclear envelope, temperature-sensitive embryonic lethality, sterility, and enhanced transgenerational RNAi inheritance.[44,45,55] MIP-1/EGGD-1 is reported to be enriched in P granules, yet the cellular localization of MIP-2/EGGD-2 in germ cells is still unclear.[44,45] Consistent with the findings of a recent study,[64] we found that MIP-2::GFP was enriched in Z granules in germ cells (Figures 2A, 2C, and 2D). LOTR-1, another LOTUS domain-containing protein, accumulated in the Z granule, as reported previously (Figures 2C and S2A).[43]

Vasa DEAD-box helicases are widespread markers of germ cells among different species.[65] *C. elegans* has four Vasa family members, namely, GLH-1, GLH-2, GLH-3, and GLH-4, all of which are associated with germ granules.[66] Among these proteins, GLH-1 and GLH-4 are required for proper association of the PGL family proteins with P granules and for the organization of germ granules.[66–68] We examined whether these proteins are enriched in the P granule. GLH-1 colocalized with WAGO-1 (Figure 2A), and GLH-2 colocalized with PGL-1 (Figure S2B), suggesting that GLH-1 and GLH-2 accumulated in the P granule. Interestingly, GLH-3 largely accumulated at distinct perinuclear foci but with slight P granule localization (Figures 2A and 2C). We further found that GLH-3 mainly colocalized with tagRFP::ZNFX-1, suggesting that GLH-3 preferentially accumulated in the Z granule (Figures 2C and 2D). Similarly, GLH-4::GFP did not colocalize with PGL-1::tagRFP but colocalized with tagRFP::ZNFX-1 (Figures 2A, 2C, and 2D). Interestingly, all four proteins contain DEAD/DEAH box helicase domains, helicase-conserved C-terminal domains, and zf-CCHC domains (Figure S3A).[69] The zf-CCHC domains are relatively small protein motifs that contain multiple finger-like protrusions that make tandem contacts with their target molecules, including RNAs and DNAs.[70,71] The protein sequences of the zf-CCHC domains of GLH-1 are largely similar to those of GLH-2 but different from those of GLH-3 or GLH-4, implying that GLH-1 and GLH-2 may bind to similar RNA molecules that are distinct from the RNA interactors of GLH-3 or GLH-4 (Figure S3B). It has been reported that sequence-encoded and composition-dependent protein-RNA interactions can control multiphasic condensate morphologies.[72] Thus, we speculate that the RNA molecules that bind to specific Vasa DEAD-box helicases may contribute to their distinct cellular localization. Alternatively, different protein interactors of these helicases may help determine their localization.

To further confirm the Z granule localization of these proteins, we examined whether their perinuclear distributions were affected by defects in Z granule assembly. PID-2/ZSP-1 regulates the morphology of Z granules without detectably affecting the morphology of P granules, *Mutator* foci, or SIMR foci.[15,56] Thus, we examined whether these four proteins were still enriched in Z granules in *pid-2* mutants. As *pid-2/zsp-1* and *deps-1* are genetically linked, we directly knocked out the *pid-2* gene in the *deps-1::gfp; tagRFP::znfx-1* animals via a dual sgRNA strategy (Figure 2E).[59] As expected, all of these proteins remained colocalized with tagRFP::ZNFX-1 in *pid-2* mutants, further suggesting that these proteins were Z granule components (Figure 2F).

piRNA processing factors accumulate in distinct germ granule compartments

piRNAs (21U-RNAs in *C. elegans*) are produced from Pol II-transcribed piRNA precursors and are subjected to a series of processing steps in the cytoplasm (Figure 3A).[73–76] Many cytoplasmic piRNA processing factors are enriched in germ granules.[21]

The PICS/PETISCO complex consists of four core subunits, namely, PICS-1/PID-3, PID-1, TOFU-6, and ERH-2.[50,77–81] The PICS/PETISCO complex stabilizes the PUCH complex and facilitates 5′ trimming of piRNA precursors.[75] We previously reported that knocking down *csr-1* and *glh-1*, two reported P granule components, failed to disrupt perinuclear PICS foci, implying that the PICS/PETISCO complex may not localize to P granules.[50] Consistent with this idea, these proteins did not colocalize but rather were adjacent to the P granule marker PGL-1 (Figure 3B). Moreover, the PICS complex did not localize to SIMR foci (marked by SIMR-1:tagRFP) or *Mutator* foci (marked by mCherry::MUT-16) (Figures S4A and S4B). We observed that all the GFP-tagged PICS complex components colocalized with tagRFP::ELLI-1, which is a marker of the E granule

Figure 2. Identification of Z granule-enriched perinuclear proteins

(A, B, and D) Fluorescence micrographs of pachytene cells that express the indicated fluorescent proteins.

(C) Quantification of colocalization between the indicated fluorescent proteins in pachytene cells (see STAR Methods). The mean is indicated by a solid black line.

(E) Sequence information of the *pid-2* allele generated via a multiple sgRNA-based CRISPR-Cas9 gene editing system.[59]

(F) Images of tagRFP::ZNFX-1 and the indicated GFP-tagged proteins in the germ cells of *pid-2(ust628)* or *pid-2(gg682)* animals.

See also Figure S3.

Please cite this article in press as: Huang et al., Compartmentalized localization of perinuclear proteins within germ granules in *C. elegans*, Developmental Cell (2024), https://doi.org/10.1016/j.devcel.2024.12.016

A

Proteins	Cellular localization	Steps	References
The PUCH complex (TOFU-1, TOFU-2 and SLFL-3/4)	Mitochondria?	5′ cleavage	ref [75]
TOFU-7	Unknown	Unknown	ref [81]
The PICS/PETISCO complex (PICS-1/PID-3, TOFU-6, ERH-2 and PID-1)	E granule	5′ and 3′ processing	refs [50, 77]
PRG-1	Z and P granules	The PIWI protein	refs [87, 88, 89]
PARN-1	Z granule	3′ trimming	ref [84]
HENN-1	P granule	2′-O-methylation	refs [95, 96, 97]

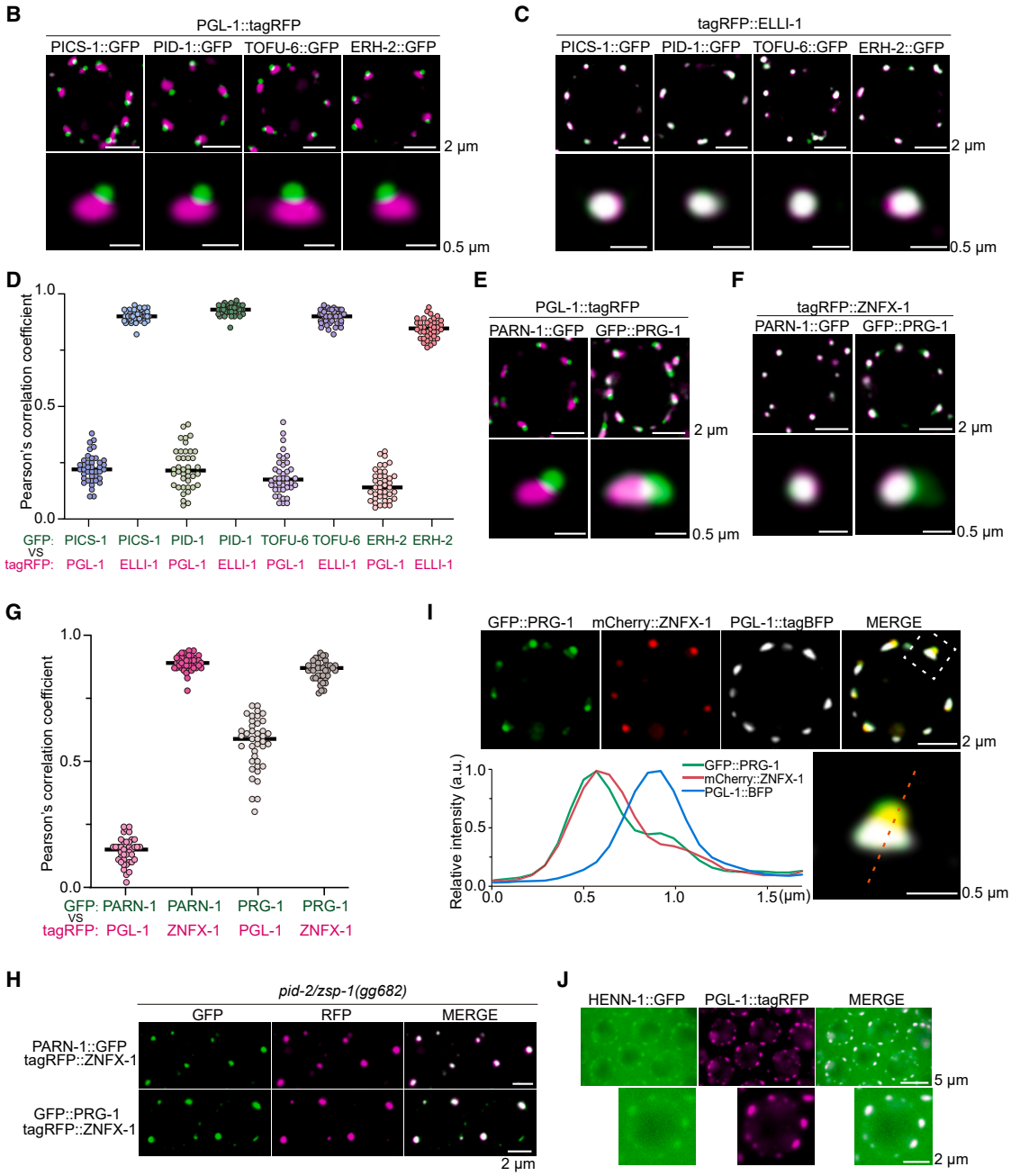

(legend on next page)

Please cite this article in press as: Huang et al., Compartmentalized localization of perinuclear proteins within germ granules in *C. elegans*, Developmental Cell (2024), https://doi.org/10.1016/j.devcel.2024.12.016

(Figure 3C). Image quantification of the spatial overlap between these fluorescence signals further revealed that the PICS complex was enriched in the E granule (Figure 3D). The LOTUS domain protein MIP-1/EGGD-1 is required for the perinuclear localization of P granules, Z granules, and *Mutator* foci.[44,45,55] However, similar to other E granule components,[28] the PICS complex remained enriched in perinuclear condensates upon depletion of MIP-1/EGGD-1 (Figures S4C and S4D). Intriguingly, IFE-3, a *C. elegans* eIF4E homolog that interacts with PID-1 and is likely involved in the 5′ maturation of piRNA precursors, whose foci have been reported to separate from PGL-1/IFE-1 foci,[77,82,83] colocalized with mCherry::CGH-1 and accumulated in the P- body (Figure S4E).

parn-1 encodes a conserved RNA exoribonuclease that trims piRNA 3′ ends.[84–86] PARN-1 did not colocalize with PGL-1 but rather colocalized with ZNFX-1, suggesting that PARN-1 accumulated in the Z granule (Figures 3E–3G). In *pid-2* mutants, PARN-1 remained colocalized with ZNFX-1 (Figure 3H).

PRG-1 is a member of the *C. elegans* PIWI family that exclusively binds to piRNAs and mediates the genome-wide surveillance of germline transcripts.[87–93] PRG-1 interacts with ZNFX-1, DEPS-1, and LOTR-1, and the typical morphology of PRG-1 condensates is regulated by both DEPS-1 and LOTR-1.[43,61,94] We found that PRG-1 accumulated in both the P and Z granules and was largely enriched in the Z granule (Figures 3E–3G). Tricolor images from animals simultaneously expressing PGL-1::tagBFP, mCherry::ZNFX-1, and GFP::PRG-1 further support the above conclusion (Figure 3I). Additionally, PRG-1 remained colocalized with ZNFX-1 in both *pid-2* and *mip-1* mutants (Figures 3H, S4F, and S4G). HENN-1 is a 2′-O-methyltransferase that methylates small RNA molecules at their 3′ terminus, including piRNAs and ERGO-1-bound 26G RNAs.[95–97] Consistent with previous reports, HENN-1 accumulated in the P granule (Figure 3J).[96]

PID-4 and PID-5 were identified as PID-2 interactors that act redundantly for piRNA sensor silencing, affect the size and appearance of Z granules, and regulate 22G RNA production and germline immortality.[56] We found that both PID-4 and PID-5 largely colocalized with tagRFP::ZNFX-1 and largely accumulated in Z granules in germ cells of both L4 and adult animals, as previously reported (Figures S4H–S4K).[56]

As piRNA processing factors are enriched in distinct subcompartments of the germ granule, we speculated that piRNA intermediates may be transported between different subcompartments and/or the cytosol. Moreover, the accumulation of piRNA processing factors or piRNA-based gene silencing factors in Z granules suggests that the Z granule may function as a key hub for piRNA biogenesis and surveillance, in addition to mediating RNAi inheritance.

DDX-19 and CSR-1 define the D granule

DDX-19, a predicted DEAD-box helicase, is a conserved mRNA export factor related to DDX19 in mammals and Dbp5p in yeast.[46] Intriguingly, DDX-19 is reported to be concentrated between the zones of PGL-1 and NPP-9 and therefore forms a tripartite architecture in L4 stage gonads and adult oogonia.[46] To further explore the formation of DDX-19 foci in *C. elegans*, we systematically examined the expression pattern and cellular localization of DDX-19::GFP in different tissues during development.

DDX-19::GFP was expressed at low levels in somatic cells but was highly expressed in germ cells and embryos (Figures S5A and S5B). In the embryos and somatic cells of hatched worms, DDX-19 was evenly distributed around the nuclear rim and mainly colocalized with the nuclear membrane protein NPP-9::mCherry (Figures S5C–S5E). In embryonic Z2/Z3 cells, DDX-19::GFP did not obviously separate from NPCs and still colocalized with NPP-9::mCherry (Figure S5F). DDX-19 foci, which are clearly separated from NPCs, can be observed in germ cells at the L1 stage (Figure S5F). DDX-19 was consistently enriched in perinuclear condensates throughout the subsequent development of germ cells in both larvae and adults (Figures S5A and S5B). Consistent with a previous report,[46] DDX-19 foci were positioned above NPCs and under P granules in germ cells (Figures 4A, 4B, and S5G). Therefore, we named the DDX-19 foci D granules. The above results suggested that the assemblage of D granules was developmentally regulated.[55] Furthermore, the loss of MIP-1/EGGD-1 disrupted the PGL-1- and WAGO-1-marked P granule but did not affect the perinuclear localized DDX-19 foci, suggesting that MIP-1/EGGD-1 was not required for the perinuclear anchoring of D granules (Figures 4C and S5H). The residual PGL-1 foci still localized adjacent to DDX-19 foci in the *mip-1/eggd-1* mutants (Figures 4D and S5H).

CSR-1 is the unique essential Argonaute protein in *C. elegans*. The genomic *csr-1* locus encodes two isoforms, CSR-1a and CSR-1b, which vary only in their N-termini.[98,99] CSR-1a is expressed during spermatogenesis and in several somatic tissues, including the intestine, and CSR-1b is expressed constitutively in the germline.[98,99] CSR-1 largely accumulates to perinuclear granules in *mip-1/eggd-1* or *glh-1;glh-4* mutants.[55,68] Here, we synchronously tagged two isoforms and focused on the cellular localization of CSR-1b in germ cells.[100] We found that CSR-1 mainly colocalized with DDX-19 yet revealed a moderate localization in the P granule (Figures 4E and 4F). Tricolor images from animals simultaneously expressing PGL-1::tagBFP, DDX-19::mCherry, and GFP::CSR-1 further supported the above conclusion (Figure 4G). The loss of MIP-1/EGGD-1 dramatically decreased the localization of CSR-1 in P granules but had a marginal, if any, effect on D granule localization (Figures 4C and 4D).

Figure 3. Subcellular localization of piRNA processing factors in *C. elegans*

(A) Summary of proteins that participate in piRNA processing in *C. elegans*.

(B, C, E, and F) Fluorescence micrographs of pachytene germ cells expressing the indicated proteins. (D and G) Quantification of colocalization between the indicated fluorescent proteins in pachytene cells (see STAR Methods). The mean is indicated by a solid black line.

(H) Images of tagRFP::ZNFX-1 and the indicated GFP-tagged proteins in the germ cells of *pid-2(ust628)* animals.

(I) Fluorescence micrographs of pachytene cells from animals expressing GFP::PRG-1, mCherry::ZNFX-1, and PGL-1::tagBFP. The intensity of the fluorescence along the dotted line was calculated by Leica Application Suite X software.

(J) Pachytene germ cells of animals that express HENN-1::GFP and PGL-1::tagRFP.

See also Figure S4.

Please cite this article in press as: Huang et al., Compartmentalized localization of perinuclear proteins within germ granules in *C. elegans*, Developmental Cell (2024), https://doi.org/10.1016/j.devcel.2024.12.016

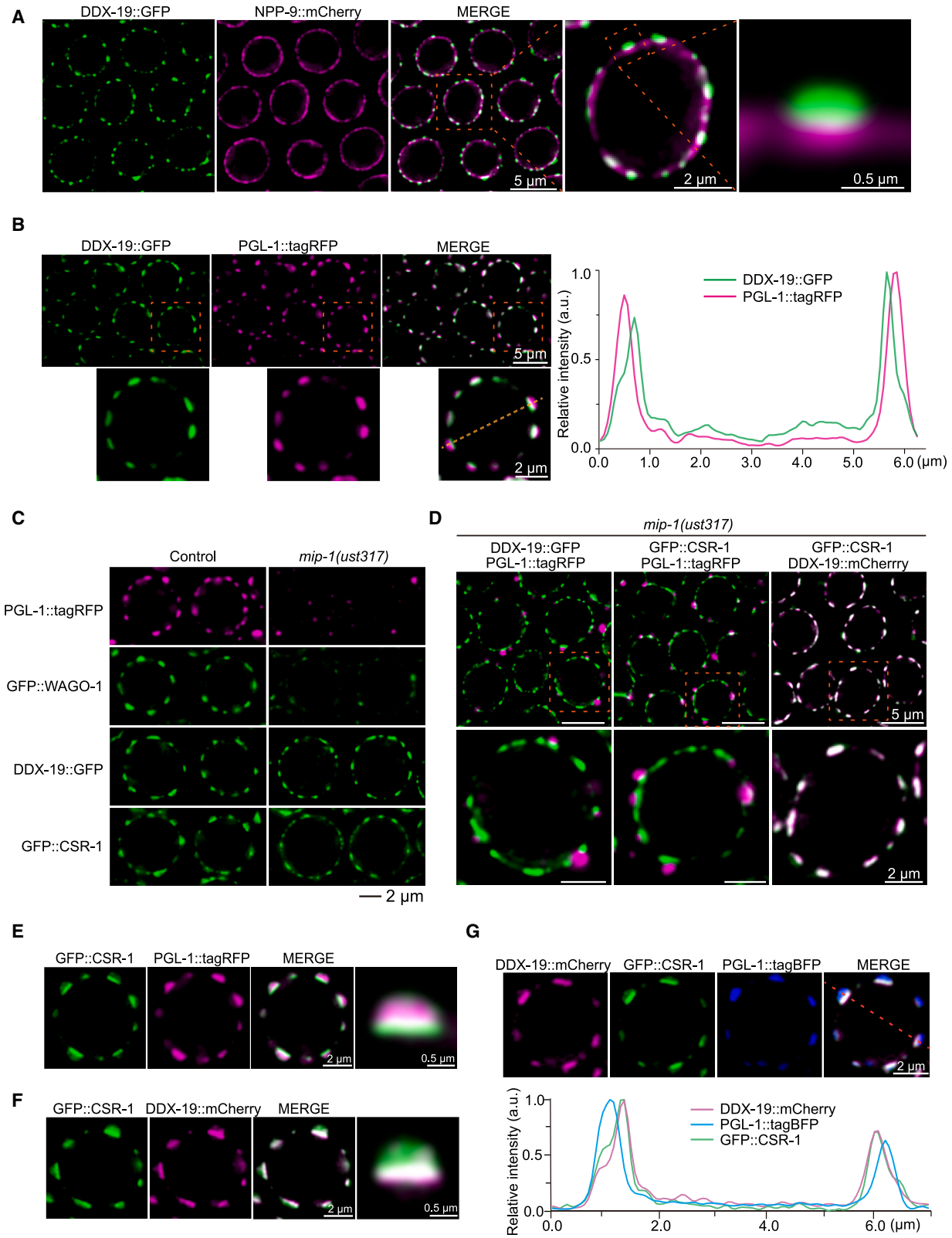

(legend on next page)

Please cite this article in press as: Huang et al., Compartmentalized localization of perinuclear proteins within germ granules in *C. elegans*, Developmental Cell (2024), https://doi.org/10.1016/j.devcel.2024.12.016

C. elegans NXF-1, the ortholog of the essential mRNA export factor NXF1/TAP in humans and Mex67p in yeast, is reported to be concentrated below P granules, whose localization at the nuclear rim is very similar to that of NPP-9.[46,101] We found that NXF-1 was localized mainly in the nucleus, as recently reported (Figure S5I).[102] Additionally, a small portion of this protein was enriched at the base of DDX-19 condensates, suggesting that perinuclear NFX-1 may be enriched in NPCs (Figure S5I).

Overall, these results extended the characterization and components of D granules and confirmed the tripartite architecture of the P granule, the D granule, and the NPC.[46]

The LOTUS domain protein MIP-1/EGGD-1 sculptures the architecture of the germ granule

Recent reports have shown that the loss of MIP-1/EGGD-1 disrupts perinuclear positioning of P granules, Z granules, and *Mutator* foci and induces their mislocalization within the adult gonad.[44,45,55] Here, we further examined whether MIP-1/EGGD-1 is required for the assembly and perinuclear localization of other germ-granule compartments. Consistently, the depletion of MIP-1/EGGD-1 resulted in the dissociation of PGL-1, ZNFX-1, and MUT-16 foci from the nucleus and the accumulation of these aggregates at the rachis (Figures 5A–5G, S6A, and S6B). Additionally, when MIP-1/EGGD-1 was deleted, the SIMR foci also largely detached from the perinuclear zone and accumulated at the rachis (Figures 5H, 5I, and S6C). However, D granules (marked by DDX-19 and CSR-1) (Figures 5J–5L, S6D, and S6E), E granules (marked by ELLI-1 and EGC-1) (Figures 5M–5O and S6F–S6H), and P-bodies (marked by CGH-1) (Figures S6I and S6J) still presented pronounced perinuclear foci. Additionally, the loss of MIP-1/EGGD-1 did not induce the generation of dissociative D and E granules in the rachis (Figures 5J, 5L, 5M, 5O, S6F, and S6H). Conversely, rachis-localized E granules (marked by ELLI-1 or EGC-1), which exist in wild-type animals,[28,47] were dramatically reduced in *mip-1/eggd-1* mutants (Figures 5M, 5O, S6F, and S6H). Since P-body proteins were also enriched as irregularly shaped aggregates in the rachis of the germ line in wild-type animals, it is unclear whether P-bodies were altered in the rachis upon the depletion of MIP-1/EGGD-1 (Figure S6I).

We further tested the colocalization of different germ-granule compartments to examine whether these perinuclear condensates remain immiscible in *mip-1/eggd-1* mutants. The residual PGL-1::tagRFP, GFP::ZNFX-1, mCherry::MUT-16, and SIMR-1::tagRFP remained separated from each other in *mip-1/eggd-1* mutants (Figures 6A and 6B).[55] Interestingly, the depletion of MIP-1/EGGD-1 induced the colocalization of ELLI-1 foci and DDX-19 foci, indicating a likely disruption of immiscibility between the D and E granules (Figures 6A, 6B, and S7A). Alternatively, the spatial distance of the D and E granules may be so small in *mip-1* mutants that it exceeds the resolution limit of optical microscopy (200 nm), making it hard to distinguish between these two condensates. D granules remained located above NPCs in *mip-1* mutants, suggesting that MIP-1 is not required for driving the incompatibility between D granules and NPCs (Figure S7B). The P-body marker CGH-1 still accumulated in the perinuclear region and did not fuse with D granules in *mip-1* mutants (Figures 6A and 6B).

Overall, these data suggest that MIP-1/EGGD-1 sculptures the architecture of the germ granule by exerting distinct regulatory effects on different subcompartments, including promoting the perinuclear anchoring of the P, Z, M, and S compartments and regulating the immiscibility between the D and E compartments.

DISCUSSION

Here, via CRISPR-Cas9 technology, we systematically tagged perinuclear proteins with fluorescent tags and examined their localization within germ granules in pachytene cells. We found that these proteins were enriched in specialized germ-granule compartments. In particular, proteins involved in particular piRNA processing steps are enclosed in different subcompartments. We also extended the characterization of the D granule. Finally, we found that the LOTUS domain protein MIP-1/EGGD-1 regulated the multilayered organization of the germ granule. Together, these data extend our understanding of the germ-granule architecture. Moreover, the library of nematode strains reported in this study further improved the available tools for studying *C. elegans* germ granules. These strains, together with many other valuable nematode strains, which were constructed by other *C. elegans* groups and have been widely shared around the world, provide powerful resources for further investigating the compartmentalization and functions of *C. elegans* germ granules.

When studying how perinuclear localization coordinates the biological functions of particular proteins, the following issues may need to be considered. (1) The architecture of the germ granule may be reorganized during development. For example, in the germline progenitor cells of early embryos, Z granules fuse with P granules, and after the 100-cell stage of embryonic development, Z granules demix into discrete condensates, distinct from P granules.[14] Moreover, a recent study identified a sperm-specific germ granule, the PEI granule, that mediates paternal epigenetic inheritance during spermatogenesis.[103] Thus, a comprehensive understanding of the localization patterns of

Figure 4. DDX-19 and CSR-1 are enriched in D granules

(A) Fluorescence images of pachytene cells expressing DDX-19::GFP and NPP-9::mCherry. NPP-9 is a putative homolog of UNP358 in humans and forms part of the NPC cytoplasmic fibrils.[46]

(B) Left, fluorescence micrographs of pachytene cells expressing DDX-19::GFP and PGL-1::tagRFP. Right, the fluorescence intensity along the dotted line.

(C) Images of representative meiotic germ cells from the indicated animals.

(D) Fluorescence micrographs of *mip-1/eggd-1* animals expressing the indicated proteins.

(E and F) Fluorescence micrographs of animals expressing indicated proteins.

(G) Upper, fluorescence micrographs of pachytene cells expressing DDX-19::mCherry, GFP::CSR-1, and PGL-1::tagBFP. Lower, the fluorescence intensity along the dotted line.

See also Figure S5.

Please cite this article in press as: Huang et al., Compartmentalized localization of perinuclear proteins within germ granules in *C. elegans*, Developmental Cell (2024), https://doi.org/10.1016/j.devcel.2024.12.016

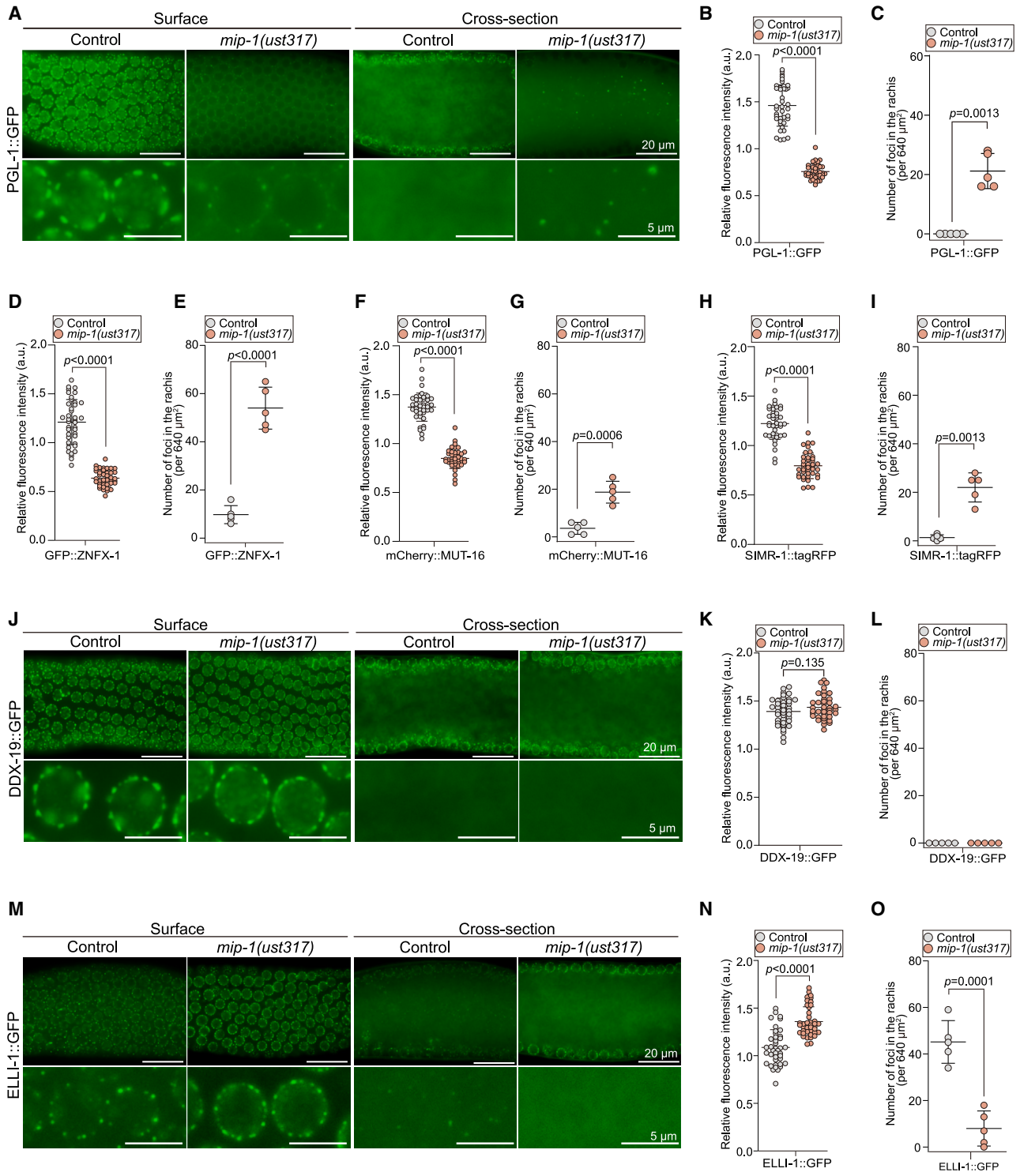

Figure 5. MIP-1/EGGD-1 exerts multiple regulatory effects on the perinuclear anchoring of different subcompartments of the germ granule

(A) Fluorescence micrographs of the surface and rachis of the germline in live adult animals expressing PGL-1::GFP in wild-type and *mip-1/eggd-1* animals.

(B) Quantification of the relative fluorescence intensity of PGL-1::GFP from the surface of the germline at the pachytene stage in the indicated animals (see STAR Methods).

(C) Quantification of the numbers of PGL-1::GFP foci in the rachis of the germline in the indicated animals (see STAR Methods).

(D, F, and H) Quantification of the relative fluorescence intensity of GFP::ZNFX-1 (D), mCherry::MUT-16 (F), and SIMR-1::tagRFP (H) from the surface of the germ line at the pachytene stage in the indicated animals.

(legend continued on next page)

perinuclear proteins during development is essential for clarifying how compartmental localization contributes to their biological functions. (2) An additional concern regarding the biological functions of compartmental positioning is the quantification of the relative enrichment of each protein in germ granules versus in the cytosol.[104] As membraneless organelles, different germ-granule compartments may constantly exchange internal substances with each other or with the cytosol.[14,41,105–107] Furthermore, *C. elegans* germ cells share a central core of the cytoplasm (the rachis) that runs through the entire germline, comprising a syncytial architecture.[108] These perinuclear proteins, which are specifically enriched in particular germ-granule compartments, may disperse in the cytosol/rachis at the same time. Proteins in the cytosol/rachis may also perform unignorable and pronounced functions. Modifying the compartmental enrichment of particular proteins by tethering methods may help elucidate the biological functions of their peculiar localization. (3) Particular germ-granule compartments may exhibit further internal hierarchical organization.[23] For example, in embryos, P granules contain at least two subcompartments: an inner core marker by PGL-1 and an outer layer marked by the intrinsically disordered protein MEG-3.[105,106] Similarly, PID-2/ZSP-1 localizes to the surface or outer periphery of Z granules and does not evenly diffuse throughout Z granules in pachytene cells, suggesting a core and surface subdivision of the Z granule.[15] In this study, the resolution limit of optical microscopy (200 nm) restricted our investigation of the inner organization of these granules. Further analysis of protein distribution within particular germ-granule compartments via high-resolution microscopy, for example, stimulated emission depletion (STED) microscopy,[15,109] may help reveal the internal hierarchical organization of these subdomains or identify uncharted subcompartments of the germ granule.

RNAs transcribed in the nucleus should pass through NPCs before being transported to the cytoplasm or the cocytoplasmic vesicles of the germline for translation.[110] Interestingly, approximately 75% of the nuclear pores in *C. elegans* germ cells are associated with germ granules.[46,111] Since D granules are concentrated between P granules and NPCs, they might act as the initial condensate to house RNPs exported from the nucleus. Consistently, DDX-19 is a predicted DEAD-box helicase related to DDX19 in mammals or Dbp5p in yeast that functions in mRNA export from the nucleus.[112–115] Thus, the D granule may participate in sorting mRNAs exported from the nucleus to other subcompartments of the germ granule. CSR-1 protects the germline transcriptome against the silencing activities of the piRNA genome surveillance pathway, further suggesting that D granules may be the initial site for the determination of RNA fate.[116,117] Deciphering the D granule proteome, for example, via TurboID-based proximity labeling,[45,118] may further help to define its biological functions.

The mechanism by which condensates form and maintain internal subcompartments is unclear. Studies on the characteristic core-shell spheroidal structure of the nucleolus reveal that differences in subcompartment surface tension, which arises from the sequence features of macromolecular components, including RNAs and proteins, may determine the immiscibility of different subcompartments and multilayered organization.[10,72,119] Similarly, these biological molecules are also essential for the formation and hierarchical organization of the germ granule in *C. elegans*.[35,41,46,120] We and others reported that the loss of MIP-1/EGGD-1 leads to extensive germ-granule remodeling.[44,45,55] How does the LOTUS domain protein MIP-1/EGGD-1 participate in the organization of germ-granule subcompartments? The LOTUS domain, which is widely conserved in eukaryotes, has been identified within several proteins, such as TDRD5, TDRD7, Oskar, and MARF1.[121,122] These proteins have also emerged as key regulators of germ-granule organization in multiple organisms.[20,22,24,123] Intriguingly, LOTUS domains reportedly have both RNA-binding activity, particularly for G-rich/G4 RNAs, and protein-binding activity, especially for RNA helicases.[121,122] Since the loss of MIP-1/EGGD-1 did not affect the perinuclear anchoring of D granules, we speculate that MIP-1/EGGD-1 may participate in the allocation of RNA molecules from the D granule to other germ-granule subcompartments, thereby resulting in the establishment of different surface tensions of distinct germ-granule subcompartments to confer immiscibility and promote spatially organized architecture. Further studies are needed to investigate the functions of LOTUS domain proteins and RNA helicases in the organization of germ-granule architecture.

Intracellular condensates are highly multicomponent systems that enclose a variety of RNP bodies in micron-scale membraneless organelles, undertaking diverse RNA processing events or sequential RNA processing reactions.[7,13,124–126] The compartmentalized structure of biomolecular condensates may provide an ingenious and efficient strategy for cells to regulate the spatial partitioning and processing of biomolecules.[8] In this study, we found that factors involved in particular piRNA processing steps were enriched in distinct germ-granule compartments. On the basis of their compartmental positioning in this study, we speculate that *C. elegans* piRNA precursors may be transported in an E-Z-P direction within the germ granule, and mature piRNAs may accumulate in both Z and P granules. Spatiotemporally partitioning sequential piRNA processing steps may promote piRNA maturation and piRNA-based gene silencing. For example, in mouse prospermatogonia (ProSg), pi bodies and piP bodies, which are often in close proximity to each other, facilitate the

(E, G, and I) Quantification of the numbers of GFP::ZNFX-1 (E), mCherry::MUT-16 (G), and SIMR-1::tagRFP (I) foci in the rachis of the germline in the indicated animals.
(J and M) Fluorescence micrographs of the surface and rachis of the germline in live adult animals expressing DDX-19::GFP (J) and ELLI-1::GFP (M) in the indicated animals.
(K and N) Quantification of the relative fluorescence intensity of DDX-19::GFP (K) and ELLI-1::GFP (N) from the surface of the germline at the pachytene stage in the indicated animals.
(L and O) Quantification of the numbers of DDX-19::GFP (L) and ELLI-1::GFP (O) foci in the rachis of the germline in the indicated animals. All data are represented as mean ± SD. A two-tailed Student's t test was performed to determine *p* values.
See also Figure S6.

Please cite this article in press as: Huang et al., Compartmentalized localization of perinuclear proteins within germ granules in *C. elegans*, Developmental Cell (2024), https://doi.org/10.1016/j.devcel.2024.12.016

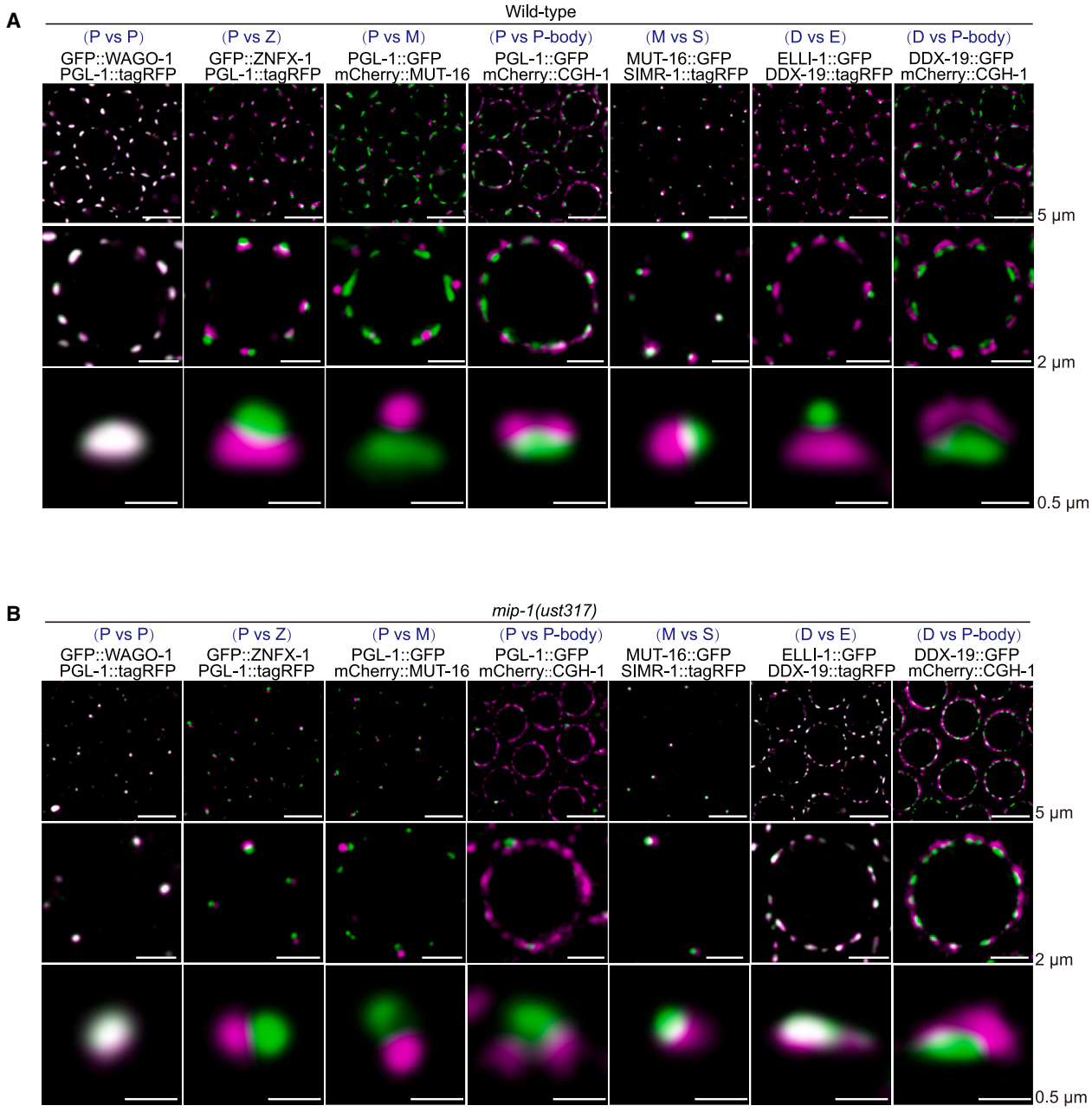

Figure 6. The LOTUS domain protein MIP-1/EGGD-1 regulates the immiscibility between D and E granules

(A and B) Fluorescence micrographs of wild-type (A) and *mip-1/eggd-1* animals (B) expressing the indicated proteins. DDX-19 and ELLI-1 largely colocalized with each other upon depletion of MIP-1/EGGD-1.

See also Figure S7.

processing of primary and secondary pre-pachytene piRNAs, respectively, and promote the silencing of transposable elements.[23,123] The proper assembly of perinuclear germ granules also functions critically to promote the fidelity of piRNA-based transcriptome surveillance in *C. elegans*.[55,67,68] However, the causal relationship between RNA metabolism and the multilayered phase structure remains controversial. Whether the compartmental positioning of these piRNA factors per se is essential for piRNA biogenesis is still largely unknown. Recent studies on the *C. elegans* nucleolar structure revealed that NUCL-1, a homolog of Nucleolin in *C. elegans*, is required for the sub-nucleolar organization of the nucleolus.[127] Yet, the loss of NUCL-1 did not elicit severe growth defects or sterility, which are usually observed in animals with defects in ribosome biogenesis,[127–131] implying that the specific architecture of the nucleolus may not be essential for the sequential processing of ribosomal RNAs in *C. elegans*, at least under normal laboratory cultivation conditions.[15] The same situation may also occur in

Please cite this article in press as: Huang et al., Compartmentalized localization of perinuclear proteins within germ granules in *C. elegans*, Developmental Cell (2024), https://doi.org/10.1016/j.devcel.2024.12.016

the sequential processing events of piRNAs, although systematic studies on the relationship between piRNA processing and germ-granule assembly are still lacking. Alternatively, the compartmental localization of piRNA processing factors may restrain the generation of mature piRNAs to maintain a proper piRNA surveillance system. Furthermore, the distinct distribution of piRNA processing factors within germ granules may provide a strategy for monitoring particular steps of piRNA processing. For example, a recent study reported that the accumulation of 3′ untrimmed piRNA precursors in *parn-1* mutants elicits the production of anti-piRNAs, which are dependent on RdRP EGO-1 and regulate the function of PRG-1 in 22G RNA production.[85] The enclosing of both the PICS and EGO complexes to E granules might contribute to this process. Further examination of piRNA biogenesis upon artificial modification of the subregional localization of piRNA processing factors may help decipher whether and how multiple immiscible condensed phases contribute to piRNA maturation.

C. elegans germ granules consist of multiple subcompartments, including but possibly not limited to the P, Z, M, S, E, and D compartments and the P-body. However, the biological significances of the multiphasic architecture of the germ granule and the localization of proteins in these germ-granule compartments remain ambiguous. As a perinuclear organelle directly bound to the NPC, the germ granule is likely the principal site of mRNA export in germ cells to sort mRNAs to their destined regulatory molecules.[21,46,132] The multiphase organization of the germ granule may provide multiple unique compartments for enriching regulatory molecules and establishing particular gene regulatory networks, especially for complex small RNA-based gene regulation pathways.[21,40] *C. elegans* proteins involved in small RNA pathways are generally enriched in germ granules in the germ line, being anchored around the nucleus.[21,28,40] Defects in germ-granule assembly are usually accompanied by disordered expression of endogenous small RNAs, leading to abnormal gene silencing events and defects in distinguishing self from non-self-nucleic acids. For example, *meg-3/4* animals produce aberrant siRNAs targeting *sid-1* and *rde-11*, which silence the expression of these two genes and consequently result in defects in the feeding RNAi response.[133–135] The same event also occurs in *egc-1* and *elli-1* mutants, in which E granule assembly is disrupted.[28,47] Moreover, *glh-1/glh-4* mutants exhibit defects in the formation of multiple perinuclear condensates and aberrant piRNA surveillance, which targets hundreds of endogenous genes.[67,68] Therefore, the positioning of proteins or RNAs within these germ-granule compartments may promote the recognition of self and non-self-nucleic acids and help suppress aberrant gene silencing events targeting endogenous genes, possibly through restraining the abnormal entry of germline genes into the polyUG/siRNA system.[104] Since polyUG RNA/siRNA cycling is self-perpetuating,[42] any stochastic or aberrant capture of germline mRNAs by this system, which could be caused by the abnormal accumulation of mRNA intermediates or the introduction of exogenous dsRNAs, may result in irreversible silencing, and the silencing effect may be continuously enhanced across generations if this system is not constrained. For example, the accumulation of aberrant 22G RNAs targeting essential genes in *prg-1* mutants,[136–138] which are pUG RNA/siRNA cycling dependent, silences corresponding mRNAs, such as histone mRNAs, resulting in progressive sterility.[138,139] Thus, the enclosing of small RNA pathway proteins within distinct perinuclear germ-granule compartments may help balance the activity of competing siRNA pathways and avoid excessive siRNA amplification in pUG RNA/siRNA cycling to protect functional transcripts from aberrant and unstoppable silencing. Alternatively, it is also possible that some subcompartments of the germ granule may be nonessential condensates that arise when particular RNP complexes exceed their solubility limit.[140,141] Developing technologies for manipulating the distribution of proteins in germ-granule compartments and the cytosol may help reveal whether and how germ-granule compartments perform their distinct functions.

Limitations of the study

In this study, we have systematically labeled perinuclear proteins with fluorescent tags and investigated their compartmental localization within germ granules in *C. elegans* pachytene cells. However, given the dynamic nature of germ-granule architecture throughout development, the compartmental localization of specific proteins may vary across different developmental stages of germ cells. Therefore, a comprehensive investigation of the localization patterns of perinuclear proteins during development is essential for elucidating their biological functions. Furthermore, comparisons between each tagged protein with markers of distinct germ-granule compartments may be insufficient to determine whether some proteins are localized across multiple compartments. Performing proteomic profiling of each compartment, such as using proximity labeling techniques, could provide deeper insights into the precise distribution of specific proteins in germ-granule compartments.

RESOURCE AVAILABILITY

Lead contact

Further information and requests for resources and reagents should be directed to and will be fulfilled by the lead contact, Shouhong Guang (sguang@ustc.edu.cn).

Materials availability

The nematode library listed in Table S1 has been deposited to CGC. All nematode strains used in this study listed in Table S2 will be shared by the lead contact upon request. Requests for additional unique reagents and resources should be directed to the lead contact.

Data and code availability

All data reported in this paper will be shared by the lead contact upon request. This paper does not report original code. The sequence information of the plasmids used for MosSCI is available from Figshare under the accession number Figshare: https://doi.org/10.6084/m9.figshare.26779972.v1. Any additional information required to reanalyze the data reported in this work is available from the lead contact upon request.

ACKNOWLEDGMENTS

We are grateful to Dr. Scott Kennedy and the members of the Guang laboratory for their comments. We are grateful to Dr. Donglei Zhang for sharing unpublished results. We are grateful to the International *C. elegans* Gene Knockout Consortium and the National Bioresource Project for providing the strains. Some strains were provided by the CGC, which is funded by the NIH Office of Research Infrastructure Programs (P40 OD010440). This work was supported by grants from the National Key R&D Program of China (2022YFA

1302700 and 2019YFA0802600), the National Natural Science Foundation of China (32230016, 32270583, 32070619, 32470633, 32400435, 2023M733425, and 32300438), the Strategic Priority Research Program of the Chinese Academy of Sciences (XDB39010600), the Research Funds of Center for Advanced Interdisciplinary Science and Biomedicine of IHM (QYPY20230021), and the Fundamental Research Funds for the Central Universities.

AUTHOR CONTRIBUTIONS

S.G. and X.C. conceptualized the research. Xiaona Huang, X.F., C.Z., Xinya Huang, S.G., and X.C. designed the research. X.C., Xiaona Huang, X.F., Y.-H.Y., D.X., and K.W. performed the research. Xiaona Huang, X.F., and X.C. contributed new reagents. X.C. and Xiaona Huang contributed images. X.C. and S.G. wrote the paper.

DECLARATION OF INTERESTS

The authors declare no competing interests.

STAR★METHODS

Detailed methods are provided in the online version of this paper and include the following:

- KEY RESOURCES TABLE
- EXPERIMENTAL MODEL AND STUDY PARTICIPANT DETAILS
  - Animal studies
- METHOD DETAILS
  - Construction of sgRNA plasmids and repair plasmids
  - CRISPR/Cas9-mediated gene deletion
  - CRISPR/Cas9-mediated gene tagging
  - Quantification of brood size
  - Microscopy
- QUANTIFICATION AND STATISTICAL ANALYSIS

SUPPLEMENTAL INFORMATION

Supplemental information can be found online at https://doi.org/10.1016/j.devcel.2024.12.016.

Received: March 25, 2024
Revised: August 26, 2024
Accepted: December 6, 2024
Published: December 31, 2024

REFERENCES

1. Shin, Y., and Brangwynne, C.P. (2017). Liquid phase condensation in cell physiology and disease. Science *357*, eaaf4382. https://doi.org/10.1126/science.aaf4382.
2. Courchaine, E.M., Lu, A., and Neugebauer, K.M. (2016). Droplet organelles? EMBO J. *35*, 1603–1612. https://doi.org/10.15252/embj.201593517.
3. Alberti, S., and Dormann, D. (2019). Liquid-Liquid Phase Separation in Disease. Annu. Rev. Genet. *53*, 171–194. https://doi.org/10.1146/annurev-genet-112618-043527.
4. Banani, S.F., Lee, H.O., Hyman, A.A., and Rosen, M.K. (2017). Biomolecular condensates: organizers of cellular biochemistry. Nat. Rev. Mol. Cell Biol. *18*, 285–298. https://doi.org/10.1038/nrm.2017.7.
5. Toretsky, J.A., and Wright, P.E. (2014). Assemblages: Functional units formed by cellular phase separation. J. Cell Biol. *206*, 579–588. https://doi.org/10.1083/jcb.201404124.
6. Standart, N., and Weil, D. (2018). P-Bodies: Cytosolic Droplets for Coordinated mRNA Storage. Trends Genet. *34*, 612–626. https://doi.org/10.1016/j.tig.2018.05.005.
7. Fare, C.M., Villani, A., Drake, L.E., and Shorter, J. (2021). Higher-order organization of biomolecular condensates. Open Biol. *11*, 210137. https://doi.org/10.1098/rsob.210137.
8. Lafontaine, D.L.J., Riback, J.A., Bascetin, R., and Brangwynne, C.P. (2021). The nucleolus as a multiphase liquid condensate. Nat. Rev. Mol. Cell Biol. *22*, 165–182. https://doi.org/10.1038/s41580-020-0272-6.
9. Yanagawa, M., and Shimobayashi, S.F. (2024). Multi-dimensional condensation of intracellular biomolecules. J. Biochem. *175*, 179–186. https://doi.org/10.1093/jb/mvad095.
10. Feric, M., Vaidya, N., Harmon, T.S., Mitrea, D.M., Zhu, L., Richardson, T.M., Kriwacki, R.W., Pappu, R.V., and Brangwynne, C.P. (2016). Coexisting Liquid Phases Underlie Nucleolar Subcompartments. Cell *165*, 1686–1697. https://doi.org/10.1016/j.cell.2016.04.047.
11. West, J.A., Mito, M., Kurosaka, S., Takumi, T., Tanegashima, C., Chujo, T., Yanaka, K., Kingston, R.E., Hirose, T., Bond, C., et al. (2016). Structural, super-resolution microscopy analysis of paraspeckle nuclear body organization. J. Cell Biol. *214*, 817–830. https://doi.org/10.1083/jcb.201601071.
12. Fei, J.Y., Jadaliha, M., Harmon, T.S., Li, I.T.S., Hua, B.Y., Hao, Q.Y., Holehouse, A.S., Reyer, M., Sun, Q.Y., Freier, S.M., et al. (2017). Quantitative analysis of multilayer organization of proteins and RNA in nuclear speckles at super resolution. J. Cell Sci. *130*, 4180–4192. https://doi.org/10.1242/jcs.206854.
13. Jain, S., Wheeler, J.R., Walters, R.W., Agrawal, A., Barsic, A., and Parker, R. (2016). ATPase-Modulated Stress Granules Contain a Diverse Proteome and Substructure. Cell *164*, 487–498. https://doi.org/10.1016/j.cell.2015.12.038.
14. Wan, G., Fields, B.D., Spracklin, G., Shukla, A., Phillips, C.M., and Kennedy, S. (2018). Spatiotemporal regulation of liquid-like condensates in epigenetic inheritance. Nature *557*, 679–683. https://doi.org/10.1038/s41586-018-0132-0.
15. Wan, G., Bajaj, L., Fields, B., Dodson, A.E., Pagano, D., Fei, Y.H., and Kennedy, S. (2021). ZSP-1 is a Z granule surface protein required for Z granule fluidity and germline immortality in *Caenorhabditis elegans*. EMBO J. *40*, e105612. https://doi.org/10.15252/embj.2020105612.
16. Shan, L., Xu, G., Yao, R.W., Luan, P.F., Huang, Y.K., Zhang, P.H., Pan, Y.H., Zhang, L., Gao, X., Li, Y., et al. (2023). Nucleolar URB1 ensures 3′ ETS rRNA removal to prevent exosome surveillance. Nature *615*, 526–534. https://doi.org/10.1038/s41586-023-05767-5.
17. Eddy, E.M. (1974). Fine structural observations on the form and distribution of nuage in germ cells of the rat. Anat. Rec. *178*, 731–757. https://doi.org/10.1002/ar.1091780406.
18. Eddy, E.M. (1975). Germ plasm and the differentiation of the germ cell line. Int. Rev. Cytol. *43*, 229–280. https://doi.org/10.1016/s0074-7696(08)60070-4.
19. Voronina, E., Seydoux, G., Sassone-Corsi, P., and Nagamori, I. (2011). RNA Granules in Germ Cells. Cold Spring Harb. Perspect. Biol. *3*, a002774. https://doi.org/10.1101/cshperspect.a002774.
20. Trcek, T., and Lehmann, R. (2019). Germ granules in Drosophila. Traffic *20*, 650–660. https://doi.org/10.1111/tra.12674.
21. Phillips, C.M., and Updike, D.L. (2022). Germ granules and gene regulation in the *Caenorhabditis elegans* germline. Genetics *220*, iyab195. https://doi.org/10.1093/genetics/iyab195.
22. Kemph, A., and Lynch, J.A. (2022). Evolution of germ plasm assembly and function among the insects. Curr. Opin. Insect Sci. *50*, 100883. https://doi.org/10.1016/j.cois.2022.100883.
23. Dodson, A.E., and Kennedy, S. (2020). Phase Separation in Germ Cells and Development. Dev. Cell *55*, 4–17. https://doi.org/10.1016/j.devcel.2020.09.004.
24. Lehmann, R. (2016). Germ Plasm Biogenesis-An Oskar-Centric Perspective. Curr. Top. Dev. Biol. *116*, 679–707. https://doi.org/10.1016/bs.ctdb.2015.11.024.
25. Mukherjee, N., and Mukherjee, C. (2021). Germ cell ribonucleoprotein granules in different clades of life: From insects to mammals. Wiley Interdiscip. Rev. RNA *12*, e1642. https://doi.org/10.1002/wrna.1642.
26. Strome, S., and Wood, W.B. (1982). Immunofluorescence visualization of germ-line-specific cytoplasmic granules in embryos, larvae, and adults

of *Caenorhabditis elegans*. Proc. Natl. Acad. Sci. USA *79*, 1558–1562. https://doi.org/10.1073/pnas.79.5.1558.

27. Du, Z., Shi, K., Brown, J.S., He, T., Wu, W.S., Zhang, Y., Lee, H.C., and Zhang, D.L. (2023). Condensate cooperativity underlies transgenerational gene silencing. Cell Rep. *42*, 112859. https://doi.org/10.1016/j.celrep.2023.112859.
28. Chen, X., Wang, K., Mufti, F.U.D., Xu, D., Zhu, C., Huang, X., Zeng, C., Jin, Q., Huang, X., Yan, Y.H., et al. (2024). Germ granule compartments coordinate specialized small RNA production. Nat. Commun. *15*, 5799. https://doi.org/10.1038/s41467-024-50027-3.
29. Brangwynne, C.P., Eckmann, C.R., Courson, D.S., Rybarska, A., Hoege, C., Gharakhani, J., Jülicher, F., and Hyman, A.A. (2009). Germline P Granules Are Liquid Droplets That Localize by Controlled Dissolution/Condensation. Science *324*, 1729–1732. https://doi.org/10.1126/science.1172046.
30. Seydoux, G. (2018). The P Granules of *C. elegans*: A Genetic Model for the Study of RNA-Protein Condensates. J. Mol. Biol. *430*, 4702–4710. https://doi.org/10.1016/j.jmb.2018.08.007.
31. Updike, D., and Strome, S. (2010). P granule assembly and function in *Caenorhabditis elegans* germ cells. J. Androl. *31*, 53–60. https://doi.org/10.2164/jandrol.109.008292.
32. Xu, F., Feng, X., Chen, X., Weng, C., Yan, Q., Xu, T., Hong, M., and Guang, S. (2018). A Cytoplasmic Argonaute Protein Promotes the Inheritance of RNAi. Cell Rep. *23*, 2482–2494. https://doi.org/10.1016/j.celrep.2018.04.072.
33. Ouyang, J.P.T., Zhang, W.L., and Seydoux, G. (2022). The conserved helicase ZNFX-1 memorializes silenced RNAs in perinuclear condensates. Nat. Cell Biol. *24*, 1129–1140. https://doi.org/10.1038/s41556-022-00940-w.
34. Zhang, C., Montgomery, T.A., Gabel, H.W., Fischer, S.E.J., Phillips, C.M., Fahlgren, N., Sullivan, C.M., Carrington, J.C., and Ruvkun, G. (2011). mut-16 and other mutator class genes modulate 22G and 26G siRNA pathways in *Caenorhabditis elegans*. Proc. Natl. Acad. Sci. USA *108*, 1201–1208. https://doi.org/10.1073/pnas.1018695108.
35. Phillips, C.M., Montgomery, T.A., Breen, P.C., and Ruvkun, G. (2012). MUT-16 promotes formation of perinuclear mutator foci required for RNA silencing in the *C. elegans* germline. Genes Dev. *26*, 1433–1444. https://doi.org/10.1101/gad.193904.112.
36. Manage, K.I., Rogers, A.K., Wallis, D.C., Uebel, C.J., Anderson, D.C., Nguyen, D.A.H., Arca, K., Brown, K.C., Cordeiro Rodrigues, R.J., de Albuquerque, B.F., et al. (2020). A tudor domain protein, SIMR-1, promotes siRNA production at piRNA-targeted mRNAs in *C. elegans*. eLife *9*, e56731. https://doi.org/10.7554/eLife.56731.
37. Chen, S.H., and Phillips, C.M. (2024). HRDE-2 drives small RNA specificity for the nuclear Argonaute protein HRDE-1. Nat. Commun. *15*, 957. https://doi.org/10.1038/s41467-024-45245-8.
38. Gallo, C.M., Munro, E., Rasoloson, D., Merritt, C., and Seydoux, G. (2008). Processing bodies and germ granules are distinct RNA granules that interact in *C. elegans* embryos. Dev. Biol. *323*, 76–87. https://doi.org/10.1016/j.ydbio.2008.07.008.
39. Cassani, M., and Seydoux, G. (2024). P-body-like condensates in the germline. Semin. Cell Dev. Biol. *157*, 24–32. https://doi.org/10.1016/j.semcdb.2023.06.010.
40. Sundby, A.E., Molnar, R.I., and Claycomb, J.M. (2021). Connecting the Dots: Linking *Caenorhabditis elegans* Small RNA Pathways and Germ Granules. Trends Cell Biol. *31*, 387–401. https://doi.org/10.1016/j.tcb.2020.12.012.
41. Uebel, C.J., Anderson, D.C., Mandarino, L.M., Manage, K.I., Aynaszyan, S., and Phillips, C.M. (2018). Distinct regions of the intrinsically disordered protein MUT-16 mediate assembly of a small RNA amplification complex and promote phase separation of Mutator foci. PLOS Genet. *14*, e1007542. https://doi.org/10.1371/journal.pgen.1007542.
42. Shukla, A., Yan, J., Pagano, D.J., Dodson, A.E., Fei, Y.H., Gorham, J., Seidman, J.G., Wickens, M., and Kennedy, S. (2020). poly(UG)-tailed RNAs in genome protection and epigenetic inheritance. Nature *582*, 283–288. https://doi.org/10.1038/s41586-020-2323-8.
43. Marnik, E.A., Almeida, M.V., Cipriani, P.G., Chung, G.R., Caspani, E., Karaulanov, E., Gan, H.H., Zinno, J., Isolehto, I.J., Kielisch, F., et al. (2022). The *Caenorhabditis elegans* TDRD5/7-like protein, LOTR-1, interacts with the helicase ZNFX-1 to balance epigenetic signals in the germline. PLOS Genet. *18*, e1010245. https://doi.org/10.1371/journal.pgen.1010245.
44. Cipriani, P.G., Bay, O., Zinno, J., Gutwein, M., Gan, H.H., Mayya, V.K., Chung, G., Chen, J.X., Fahs, H., Guan, Y., et al. (2021). Novel LOTUS-domain proteins are organizational hubs that recruit *C. elegans* Vasa to germ granules. eLife *10*, e60833. https://doi.org/10.7554/eLife.60833.
45. Price, I.F., Hertz, H.L., Pastore, B., Wagner, J., and Tang, W. (2021). Proximity labeling identifies Lotus domain proteins that promote the formation of perinuclear germ granules in *C. elegans*. eLife *10*, e72276. https://doi.org/10.7554/eLife.72276.
46. Sheth, U., Pitt, J., Dennis, S., and Priess, J.R. (2010). Perinuclear P granules are the principal sites of mRNA export in adult *C. elegans* germ cells. Development *137*, 1305–1314. https://doi.org/10.1242/dev.044255.
47. Andralojc, K.M., Campbell, A.C., Kelly, A.L., Terrey, M., Tanner, P.C., Gans, I.M., Senter-Zapata, M.J., Khokhar, E.S., and Updike, D.L. (2017). ELLI-1, a novel germline protein, modulates RNAi activity and P-granule accumulation in *Caenorhabditis elegans*. PLOS Genet. *13*, e1006611. https://doi.org/10.1371/journal.pgen.1006611.
48. Uebel, C.J., Rajeev, S., and Phillips, C.M. (2023). *Caenorhabditis elegans* germ granules are present in distinct configurations and assemble in a hierarchical manner. Development *150*, dev202284. https://doi.org/10.1242/dev.202284.
49. Kawasaki, I., Shim, Y.H., Kirchner, J., Kaminker, J., Wood, W.B., and Strome, S. (1998). PGL-1, a predicted RNA-binding component of germ granules, is essential for fertility in *C. elegans*. Cell *94*, 635–645. https://doi.org/10.1016/S0092-8674(00)81605-0.
50. Zeng, C., Weng, C., Wang, X., Yan, Y.H., Li, W.J., Xu, D., Hong, M., Liao, S., Dong, M.Q., Feng, X., et al. (2019). Functional Proteomics Identifies a PICS Complex Required for piRNA Maturation and Chromosome Segregation. Cell Rep. *27*, 3561–3572.e3. https://doi.org/10.1016/j.celrep.2019.05.076.
51. Xu, D., Chen, X., Kuang, Y., Hong, M., Xu, T., Wang, K., Huang, X., Fu, C., Ruan, K., Zhu, C., et al. (2023). rRNA intermediates coordinate the formation of nucleolar vacuoles in *C. elegans*. Cell Rep. *42*, 112915. https://doi.org/10.1016/j.celrep.2023.112915.
52. Zhang, Y., Wang, K., Yang, K., Shi, Y., and Hong, J. (2021). Insight into the interaction between the RNA helicase CGH-1 and EDC-3 and its implications. Sci. Rep. *11*, 20359. https://doi.org/10.1038/s41598-021-99919-0.
53. Davis, G.M., Tu, S.K., Anderson, J.W.T., Colson, R.N., Gunzburg, M.J., Francisco, M.A., Ray, D., Shrubsole, S.P., Sobotka, J.A., Seroussi, U., et al. (2018). The TRIM-NHL protein NHL-2 is a co-factor in the nuclear and somatic RNAi pathways in *C. elegans*. eLife *7*, e35478. https://doi.org/10.7554/eLife.35478.
54. Uebel, C.J., Manage, K.I., and Phillips, C.M. (2021). SIMR foci are found in the progenitor germ cells of *C. elegans* embryos. MicroPubl. Biol. *2021*, 374. https://doi.org/10.17912/micropub.biology.000374.
55. Price, I.F., Wagner, J.A., Pastore, B., Hertz, H.L., and Tang, W. (2023). *C. elegans* germ granules sculpt both germline and somatic RNAome. Nat. Commun. *14*, 5965. https://doi.org/10.1038/s41467-023-41556-4.
56. Placentino, M., de Jesus Domingues, A.M.D., Schreier, J., Dietz, S., Hellmann, S., de Albuquerque, B.F.M., Butter, F., and Ketting, R.F. (2021). Intrinsically disordered protein PID-2 modulates Z granules and is required for heritable piRNA-induced silencing in the *Caenorhabditis elegans* embryo. EMBO J. *40*, e105280. https://doi.org/10.15252/embj.2020105280.
57. Uebel, C., and Phillips, C. (2019). Phase-separated protein dynamics are affected by fluorescent tag choice. MicroPubl. Biol. *2019*, 143. https://doi.org/10.17912/micropub.biology.000143.

58. Kawasaki, I., Amiri, A., Fan, Y., Meyer, N., Dunkelbarger, S., Motohashi, T., Karashima, T., Bossinger, O., and Strome, S. (2004). The PGL family proteins associate with germ granules and function redundantly in *Caenorhabditis elegans* germline development. Genetics *167*, 645–661. https://doi.org/10.1534/genetics.103.023093.

59. Chen, X., Xu, F., Zhu, C., Ji, J., Zhou, X., Feng, X., and Guang, S. (2014). Dual sgRNA-directed gene knockout using CRISPR/Cas9 technology in *Caenorhabditis elegans*. Sci. Rep. *4*, 7581. https://doi.org/10.1038/srep07581.

60. Gu, W.F., Shirayama, M., Conte, D., Vasale, J., Batista, P.J., Claycomb, J.M., Moresco, J.J., Youngman, E.M., Keys, J., Stoltz, M.J., et al. (2009). Distinct argonaute-mediated 22G-RNA pathways direct genome surveillance in the *C. elegans* germline. Mol. Cell *36*, 231–244. https://doi.org/10.1016/j.molcel.2009.09.020.

61. Suen, K.M., Braukmann, F., Butler, R., Bensaddek, D., Akay, A., Lin, C.C., Milonaitytė, D., Doshi, N., Sapetschnig, A., Lamond, A., et al. (2020). DEPS-1 is required for piRNA-dependent silencing and PIWI condensate organisation in *Caenorhabditis elegans*. Nat. Commun. *11*, 4242. https://doi.org/10.1038/s41467-020-18089-1.

62. Houri-Ze'evi, L., Korem, Y., Sheftel, H., Faigenbloom, L., Toker, I.A., Dagan, Y., Awad, L., Degani, L., Alon, U., and Rechavi, O. (2016). A Tunable Mechanism Determines the Duration of the Transgenerational Small RNA Inheritance in *C. elegans*. Cell *165*, 88–99. https://doi.org/10.1016/j.cell.2016.02.057.

63. Spike, C.A., Bader, J., Reinke, V., and Strome, S. (2008). DEPS-1 promotes P-granule assembly and RNA interference in *C. elegans* germ cells. Development *135*, 983–993. https://doi.org/10.1242/dev.015552.

64. Zhao, C., Cai, S., Shi, R., Li, X., Deng, B., Li, R., Yang, S., Huang, J., Liang, Y., Lu, P., et al. (2024). HERD-1 mediates multiphase condensate immiscibility to regulate small RNA-driven transgenerational epigenetic inheritance. Nat. Cell Biol. *26*, 1958–1970. https://doi.org/10.1038/s41556-024-01514-8.

65. Gustafson, E.A., and Wessel, G.M. (2010). Vasa genes: Emerging roles in the germ line and in multipotent cells. BioEssays *32*, 626–637. https://doi.org/10.1002/bies.201000001.

66. Spike, C., Meyer, N., Racen, E., Orsborn, A., Kirchner, J., Kuznicki, K., Yee, C., Bennett, K., and Strome, S. (2008). Genetic analysis of the *Caenorhabditis elegans* GLH family of P-granule proteins. Genetics *178*, 1973–1987. https://doi.org/10.1534/genetics.107.083469.

67. Chen, W.J., Brown, J.S., He, T., Wu, W.S., Tu, S.K., Weng, Z.P., Zhang, D.L., and Lee, H.C. (2022). GLH/VASA helicases promote germ granule formation to ensure the fidelity of piRNA-mediated transcriptome surveillance. Nat. Commun. *13*, 5306. https://doi.org/10.1038/s41467-022-32880-2.

68. Dai, S., Tang, X., Li, L., Ishidate, T., Ozturk, A.R., Chen, H., Dude, A.L., Yan, Y.H., Dong, M.Q., Shen, E.Z., et al. (2022). A family of *C. elegans* VASA homologs control Argonaute pathway specificity and promote transgenerational silencing. Cell Rep. *40*, 111265. https://doi.org/10.1016/j.celrep.2022.111265.

69. Paysan-Lafosse, T., Blum, M., Chuguransky, S., Grego, T., Pinto, B.L., Salazar, G.A., Bileschi, M.L., Bork, P., Bridge, A., Colwell, L., et al. (2023). InterPro in 2022. Nucleic Acids Res. *51*, D418–D427. https://doi.org/10.1093/nar/gkac993.

70. Wang, Y.S., Yu, Y., Pang, Y.D., Yu, H.J., Zhang, W.Q., Zhao, X., and Yu, J.X. (2021). The distinct roles of zinc finger CCHC-type (ZCCHC) superfamily proteins in the regulation of RNA metabolism. RNA Biol. *18*, 2107–2126. https://doi.org/10.1080/15476286.2021.1909320.

71. Benhalevy, D., Gupta, S.K., Danan, C.H., Ghosal, S., Sun, H.W., Kazemier, H.G., Paeschke, K., Hafner, M., and Juranek, S.A. (2017). The Human CCHC-type Zinc Finger Nucleic Acid-Binding Protein Binds G-Rich Elements in Target mRNA Coding Sequences and Promotes Translation. Cell Rep. *18*, 2979–2990. https://doi.org/10.1016/j.celrep.2017.02.080.

72. Kaur, T., Raju, M., Alshareedah, I., Davis, R.B., Potoyan, D.A., and Banerjee, P.R. (2021). Sequence-encoded and composition-dependent protein-RNA interactions control multiphasic condensate morphologies. Nat. Commun. *12*, 872. https://doi.org/10.1038/s41467-021-21089-4.

73. Ketting, R.F., and Cochella, L. (2021). Concepts and functions of small RNA pathways in *C. elegans*. Curr. Top. Dev. Biol. *144*, 45–89. https://doi.org/10.1016/bs.ctdb.2020.08.002.

74. Weng, C., Kosalka, J., Berkyurek, A.C., Stempor, P., Feng, X., Mao, H., Zeng, C., Li, W.J., Yan, Y.H., Dong, M.Q., et al. (2019). The USTC co-opts an ancient machinery to drive piRNA transcription in *C. elegans*. Genes Dev. *33*, 90–102. https://doi.org/10.1101/gad.319293.118.

75. Podvalnaya, N., Bronkhorst, A.W., Lichtenberger, R., Hellmann, S., Nischwitz, E., Falk, T., Karaulanov, E., Butter, F., Falk, S., and Ketting, R.F. (2023). piRNA processing by a trimeric Schlafen-domain nuclease. Nature *622*, 402–409. https://doi.org/10.1038/s41586-023-06588-2.

76. Huang, X., Cheng, P., Weng, C., Xu, Z., Zeng, C., Xu, Z., Chen, X., Zhu, C., Guang, S., and Feng, X. (2021). A chromodomain protein mediates heterochromatin-directed piRNA expression. Proc. Natl. Acad. Sci. USA *118*, e2103723118. https://doi.org/10.1073/pnas.2103723118.

77. Cordeiro Rodrigues, R.J., de Jesus Domingues, A.M., Hellmann, S., Dietz, S., de Albuquerque, B.F.M., Renz, C., Ulrich, H.D., Sarkies, P., Butter, F., and Ketting, R.F. (2019). PETISCO is a novel protein complex required for 21U RNA biogenesis and embryonic viability. Genes Dev. *33*, 857–870. https://doi.org/10.1101/gad.322446.118.

78. Wang, X., Zeng, C., Liao, S., Zhu, Z., Zhang, J., Tu, X., Yao, X., Feng, X., Guang, S., and Xu, C. (2021). Molecular basis for PICS-mediated piRNA biogenesis and cell division. Nat. Commun. *12*, 5595. https://doi.org/10.1038/s41467-021-25896-7.

79. Perez-Borrajero, C., Podvalnaya, N., Holleis, K., Lichtenberger, R., Karaulanov, E., Simon, B., Basquin, J., Hennig, J., Ketting, R.F., and Falk, S. (2021). Structural basis of PETISCO complex assembly during piRNA biogenesis in *C. elegans*. Genes Dev. *35*, 1304–1323. https://doi.org/10.1101/gad.348648.121.

80. de Albuquerque, B.F.M., Luteijn, M.J., Cordeiro Rodrigues, R.J.C., van Bergeijk, P., Waaijers, S., Kaaij, L.J.T., Klein, H., Boxem, M., and Ketting, R.F. (2014). PID-1 is a novel factor that operates during 21U-RNA biogenesis in *Caenorhabditis elegans*. Genes Dev. *28*, 683–688. https://doi.org/10.1101/gad.238220.114.

81. Goh, W.S.S., Seah, J.W.E., Harrison, E.J., Chen, C., Hammell, C.M., and Hannon, G.J. (2014). A genome-wide RNAi screen identifies factors required for distinct stages of *C. elegans* piRNA biogenesis. Genes Dev. *28*, 797–807. https://doi.org/10.1101/gad.235622.113.

82. Huggins, H.P., Subash, J.S., Stoffel, H., Henderson, M.A., Hoffman, J.L., Buckner, D.S., SenGupta, M.S., Boag, P.R., Lee, M.H., and Keiper, B.D. (2020). Distinct roles of two eIF4E isoforms in the germline of *Caenorhabditis elegans*. J. Cell Sci. *133*, jcs237990. https://doi.org/10.1242/jcs.237990.

83. Gajjar, G., Huggins, H.P., Kim, E.S., Huang, W., Bonnet, F.X., Updike, D.L., and Keiper, B.D. (2024). Two germ granule eIF4E isoforms reside in different mRNPs to hand off *C elegans* mRNAs from translational repression to activation. Preprint at bioRxiv. https://doi.org/10.1101/2024.05.24.595216.

84. Tang, W., Tu, S., Lee, H.C., Weng, Z.P., and Mello, C.C. (2016). The RNase PARN-1 Trims piRNA 3' Ends to Promote Transcriptome Surveillance in *C. elegans*. Cell *164*, 974–984. https://doi.org/10.1016/j.cell.2016.02.008.

85. Pastore, B., Hertz, H.L., and Tang, W. (2024). Pre-piRNA trimming safeguards piRNAs against erroneous targeting by RNA-dependent RNA polymerase. Cell Rep. *43*, 113692. https://doi.org/10.1016/j.celrep.2024.113692.

86. Pastore, B., Hertz, H.L., Price, I.F., and Tang, W. (2021). pre-piRNA trimming and 2′-O-methylation protect piRNAs from 3′ tailing and degradation in *C. elegans*. Cell Rep. *36*, 109640. https://doi.org/10.1016/j.celrep.2021.109640.

87. Batista, P.J., Ruby, J.G., Claycomb, J.M., Chiang, R., Fahlgren, N., Kasschau, K.D., Chaves, D.A., Gu, W.F., Vasale, J.J., Duan, S.H., et al. (2008). PRG-1 and 21U-RNAs interact to form the piRNA complex

required for fertility in *C. elegans*. Mol. Cell *31*, 67–78. https://doi.org/10.1016/j.molcel.2008.06.002.

88. Das, P.P., Bagijn, M.P., Goldstein, L.D., Woolford, J.R., Lehrbach, N.J., Sapetschnig, A., Buhecha, H.R., Gilchrist, M.J., Howe, K.L., Stark, R., et al. (2008). Piwi and piRNAs act upstream of an endogenous siRNA pathway to suppress Tc3 transposon mobility in the *Caenorhabditis elegans* germline. Mol. Cell *31*, 79–90. https://doi.org/10.1016/j.molcel.2008.06.003.
89. Wang, G., and Reinke, V. (2008). A *C. elegans* Piwi, PRG-1, regulates 21U-RNAs during spermatogenesis. Curr. Biol. *18*, 861–867. https://doi.org/10.1016/j.cub.2008.05.009.
90. Shirayama, M., Seth, M., Lee, H.C., Gu, W.F., Ishidate, T., Conte, D., and Mello, C.C. (2012). piRNAs Initiate an Epigenetic Memory of Nonself RNA in the *C. elegans* Germline. Cell *150*, 65–77. https://doi.org/10.1016/j.cell.2012.06.015.
91. Luteijn, M.J., van Bergeijk, P., Kaaij, L.J.T., Almeida, M.V., Roovers, E.F., Berezikov, E., and Ketting, R.F. (2012). Extremely stable Piwi-induced gene silencing in *Caenorhabditis elegans*. EMBO J. *31*, 3422–3430. https://doi.org/10.1038/emboj.2012.213.
92. Lee, H.C., Gu, W.F., Shirayama, M., Youngman, E., Conte, D., and Mello, C.C. (2012). *C. elegans* piRNAs Mediate the genome-wide Surveillance of germline Transcripts. Cell *150*, 78–87. https://doi.org/10.1016/j.cell.2012.06.016.
93. Ashe, A., Sapetschnig, A., Weick, E.M., Mitchell, J., Bagijn, M.P., Cording, A.C., Doebley, A.L., Goldstein, L.D., Lehrbach, N.J., Le Pen, J., et al. (2012). piRNAs Can Trigger a Multigenerational Epigenetic Memory in the Germline of *C. elegans*. Cell *150*, 88–99. https://doi.org/10.1016/j.cell.2012.06.018.
94. Ishidate, T., Ozturk, A.R., Durning, D.J., Sharma, R., Shen, E.Z., Chen, H., Seth, M., Shirayama, M., and Mello, C.C. (2018). ZNFX-1 Functions within Perinuclear Nuage to Balance Epigenetic Signals. Mol. Cell *70*, 639–649.e6. https://doi.org/10.1016/j.molcel.2018.04.009.
95. Billi, A.C., Alessi, A.F., Khivansara, V., Han, T., Freeberg, M., Mitani, S., and Kim, J.K. (2012). The *Caenorhabditis elegans* HEN1 Ortholog, HENN-1, Methylates and Stabilizes Select Subclasses of Germline Small RNAs. PLOS Genet. *8*, e1002617. https://doi.org/10.1371/journal.pgen.1002617.
96. Kamminga, L.M., van Wolfswinkel, J.C., Luteijn, M.J., Kaaij, L.J.T., Bagijn, M.P., Sapetschnig, A., Miska, E.A., Berezikov, E., and Ketting, R.F. (2012). Differential impact of the HEN1 homolog HENN-1 on 21U and 26G RNAs in the germline of *Caenorhabditis elegans*. PLOS Genet. *8*, e1002702. https://doi.org/10.1371/journal.pgen.1002702.
97. Montgomery, T.A., Rim, Y.S., Zhang, C., Dowen, R.H., Phillips, C.M., Fischer, S.E.J., and Ruvkun, G. (2012). PIWI associated siRNAs and piRNAs specifically require the *Caenorhabditis elegans* HEN1 ortholog *henn-1*. PLOS Genet. *8*, e1002616. https://doi.org/10.1371/journal.pgen.1002616.
98. Charlesworth, A.G., Seroussi, U., Lehrbach, N.J., Renaud, M.S., Sundby, A.E., Molnar, R.I., Lao, R.X., Willis, A.R., Woock, J.R., Aber, M.J., et al. (2021). Two isoforms of the essential *C. elegans* Argonaute CSR-1 differentially regulate sperm and oocyte fertility. Nucleic Acids Res. *49*, 8836–8865. https://doi.org/10.1093/nar/gkab619.
99. Nguyen, D.A.H., and Phillips, C.M. (2021). Arginine methylation promotes siRNA-binding specificity for a spermatogenesis-specific isoform of the Argonaute protein CSR-1. Nat. Commun. *12*, 4212. https://doi.org/10.1038/s41467-021-24526-6.
100. Gerson-Gurwitz, A., Wang, S., Sathe, S., Green, R., Yeo, G.W., Oegema, K., and Desai, A. (2016). A Small RNA-Catalytic Argonaute Pathway Tunes Germline Transcript Levels to Ensure Embryonic Divisions. Cell *165*, 396–409. https://doi.org/10.1016/j.cell.2016.02.040.
101. Tan, W., Zolotukhin, A.S., Bear, J., Patenaude, D.J., and Felber, B.K. (2000). The mRNA export in *Caenorhabditis elegans* is mediated by Ce-NXF-1, an ortholog of human TAP/NXF and Saccharomyces cerevisiae Mex67p. Rna *6*, 1762–1772. https://doi.org/10.1017/s1355838200000832. https://rnajournal.cshlp.org/content/6/12/1762.
102. Zheleva, A., Gómez-Orte, E., Sáenz-Narciso, B., Ezcurra, B., Kassahun, H., de Toro, M., Miranda-Vizuete, A., Schnabel, R., Nilsen, H., and Cabello, J. (2019). Reduction of mRNA export unmasks different tissue sensitivities to low mRNA levels during *Caenorhabditis elegans* development. PLOS Genet. *15*, e1008338. https://doi.org/10.1371/journal.pgen.1008338.
103. Schreier, J., Dietz, S., Boermel, M., Oorschot, V., Seistrup, A.S., de Jesus Domingues, A.M.D., Bronkhorst, A.W., Nguyen, D.A.H., Phillis, S., Gleason, E.J., et al. (2022). Membrane-associated cytoplasmic granules carrying the Argonaute protein WAGO-3 enable paternal epigenetic inheritance in *Caenorhabditis elegans*. Nat. Cell Biol. *24*, 217–229. https://doi.org/10.1038/s41556-021-00827-2.
104. Ouyang, J.P.T., and Seydoux, G. (2022). Nuage condensates: accelerators or circuit breakers for sRNA silencing pathways? Rna *28*, 58–66. https://doi.org/10.1261/rna.079003.121.
105. Wang, J.T., Smith, J., Chen, B.C., Schmidt, H., Rasoloson, D., Paix, A., Lambrus, B.G., Calidas, D., Betzig, E., and Seydoux, G. (2014). Regulation of RNA granule dynamics by phosphorylation of serine-rich, intrinsically disordered proteins in *C. elegans*. eLife *3*, e04591. https://doi.org/10.7554/eLife.04591.
106. Putnam, A., Cassani, M., Smith, J., and Seydoux, G. (2019). A gel phase promotes condensation of liquid P granules in *Caenorhabditis elegans* embryos. Nat. Struct. Mol. Biol. *26*, 220–226. https://doi.org/10.1038/s41594-019-0193-2.
107. Fritsch, A.W., Diaz-Delgadillo, A.F., Adame-Arana, O., Hoege, C., Mittasch, M., Kreysing, M., Leaver, M., Hyman, A.A., Jülicher, F., and Weber, C.A. (2021). Local thermodynamics govern formation and dissolution of *Caenorhabditis elegans* P granule condensates. Proc. Natl. Acad. Sci. USA *118*, e2102772118. https://doi.org/10.1073/pnas.2102772118.
108. Amini, R., Goupil, E., Labella, S., Zetka, M., Maddox, A.S., Labbé, J.C., and Chartier, N.T. (2014). *C. elegans* Anillin proteins regulate intercellular bridge stability and germline syncytial organization. J. Cell Biol. *206*, 129–143. https://doi.org/10.1083/jcb.201310117.
109. Westphal, V., Rizzoli, S.O., Lauterbach, M.A., Kamin, D., Jahn, R., and Hell, S.W. (2008). Video-rate far-field optical nanoscopy dissects synaptic vesicle movement. Science *320*, 246–249. https://doi.org/10.1126/science.1154228.
110. Cohen-Fix, O., and Askjaer, P. (2017). Cell Biology of the *Caenorhabditis elegans* Nucleus. Genetics *205*, 25–59. https://doi.org/10.1534/genetics.116.197160.
111. Pitt, J.N., Schisa, J.A., and Priess, J.R. (2000). P Granules in the germ cells of *Caenorhabditis elegans* adults are associated with clusters of nuclear pores and contain RNA. Dev. Biol. *219*, 315–333. https://doi.org/10.1006/dbio.2000.9607.
112. Snay-Hodge, C.A., Colot, H.V., Goldstein, A.L., and Cole, C.N. (1998). Dbp5p/Rat8p is a yeast nuclear pore-associated DEAD-box protein essential for RNA export. EMBO J. *17*, 2663–2676. https://doi.org/10.1093/emboj/17.9.2663.
113. Schmitt, C., von Kobbe, C., Bachi, A., Panté, N., Rodrigues, J.P., Boscheron, C., Rigaut, G., Wilm, M., Séraphin, B., Carmo-Fonseca, M., et al. (1999). Dbp5, a DEAD-box protein required for mRNA export, is recruited to the cytoplasmic fibrils of nuclear pore complex via a conserved interaction with CAN/Nup159p. EMBO J. *18*, 4332–4347. https://doi.org/10.1093/emboj/18.15.4332.
114. Weirich, C.S., Erzberger, J.P., Berger, J.M., and Weis, K. (2004). The N-terminal domain of Nup159 forms a β-propeller that functions in mRNA export by tethering the helicase Dbp5 to the nuclear pore. Mol. Cell *16*, 749–760. https://doi.org/10.1016/j.molcel.2004.10.032.
115. Napetschnig, J., Kassube, S.A., Debler, E.W., Wong, R.W., Blobel, G., and Hoelz, A. (2009). Structural and functional analysis of the interaction between the nucleoporin Nup214 and the DEAD-box helicase Ddx19. Proc. Natl. Acad. Sci. USA *106*, 3089–3094. https://doi.org/10.1073/pnas.0813267106.

116. Seth, M., Shirayama, M., Gu, W.F., Ishidate, T., Conte, D., and Mello, C.C. (2013). The *C. elegans* CSR-1 Argonaute Pathway Counteracts Epigenetic Silencing to Promote Germline Gene Expression. Dev. Cell *27*, 656–663. https://doi.org/10.1016/j.devcel.2013.11.014.

117. Wedeles, C.J., Wu, M.Z., and Claycomb, J.M. (2013). Protection of germline gene expression by the *C. elegans* Argonaute CSR-1. Dev. Cell *27*, 664–671. https://doi.org/10.1016/j.devcel.2013.11.016.

118. Branon, T.C., Bosch, J.A., Sanchez, A.D., Udeshi, N.D., Svinkina, T., Carr, S.A., Feldman, J.L., Perrimon, N., and Ting, A.Y. (2018). Efficient proximity labeling in living cells and organisms with TurboID. Nat. Biotechnol. *36*, 880–887. https://doi.org/10.1038/nbt.4201.

119. Niepielko, M.G., Eagle, W.V.I., and Gavis, E.R. (2018). Stochastic Seeding Coupled with mRNA Self-Recruitment Generates Heterogeneous Drosophila Germ Granules. Curr. Biol. *28*, 1872–1881.e3. https://doi.org/10.1016/j.cub.2018.04.037.

120. Uebel, C.J., Agbede, D., Wallis, D.C., and Phillips, C.M. (2020). Mutator Foci Are Regulated by Developmental Stage, RNA, and the Germline Cell Cycle in *Caenorhabditis elegans*. G3 (Bethesda) *10*, 3719–3728. https://doi.org/10.1534/g3.120.401514.

121. Jeske, M., Müller, C.W., and Ephrussi, A. (2017). The LOTUS domain is a conserved DEAD-box RNA helicase regulator essential for the recruitment of Vasa to the germ plasm and nuage. Genes Dev. *31*, 939–952. https://doi.org/10.1101/gad.297051.117.

122. Kubíková, J., Reinig, R., Salgania, H.K., and Jeske, M. (2020). LOTUS-domain proteins - developmental effectors from a molecular perspective. Biol. Chem. *402*, 7–23. https://doi.org/10.1515/hsz-2020-0270.

123. Tanaka, T., Hosokawa, M., Vagin, V.V., Reuter, M., Hayashi, E., Mochizuki, A.L., Kitamura, K., Yamanaka, H., Kondoh, G., Okawa, K., et al. (2011). Tudor domain containing 7 (Tdrd7) is essential for dynamic ribonucleoprotein (RNP) remodeling of chromatoid bodies during spermatogenesis. Proc. Natl. Acad. Sci. USA *108*, 10579–10584. https://doi.org/10.1073/pnas.1015447108.

124. Khong, A., Matheny, T., Jain, S., Mitchell, S.F., Wheeler, J.R., and Parker, R. (2017). The Stress Granule Transcriptome Reveals Principles of mRNA Accumulation in Stress Granules. Mol. Cell *68*, 808–820.e5. https://doi.org/10.1016/j.molcel.2017.10.015.

125. Markmiller, S., Soltanieh, S., Server, K.L., Mak, R., Jin, W.H., Fang, M.Y., Luo, E.C., Krach, F., Yang, D.J., Sen, A., et al. (2018). Context-Dependent and Disease-Specific Diversity in Protein Interactions within Stress Granules. Cell *172*, 590–604.e13. https://doi.org/10.1016/j.cell.2017.12.032.

126. Youn, J.Y., Dunham, W.H., Hong, S.J., Knight, J.D.R., Bashkurov, M., Chen, G.I., Bagci, H., Rathod, B., MacLeod, G., Eng, S.W.M., et al. (2018). High-Density Proximity Mapping Reveals the Subcellular Organization of mRNA-Associated Granules and Bodies. Mol. Cell *69*, 517–532.e11. https://doi.org/10.1016/j.molcel.2017.12.020.

127. Spaulding, E.L., Feidler, A.M., Cook, L.A., and Updike, D.L. (2022). RG/RGG repeats in the *C. elegans* homologs of Nucleolin and GAR1 contribute to sub-nucleolar phase separation. Nat. Commun. *13*, 6585. https://doi.org/10.1038/s41467-022-34225-5.

128. Voutev, R., Killian, D.J., Ahn, J.H., and Hubbard, E.J.A. (2006). Alterations in ribosome biogenesis cause specific defects in *C. elegans* hermaphrodite gonadogenesis. Dev. Biol. *298*, 45–58. https://doi.org/10.1016/j.ydbio.2006.06.011.

129. Saijou, E., Fujiwara, T., Suzaki, T., Inoue, K., and Sakamoto, H. (2004). RBD-1, a nucleolar RNA-binding protein, is essential for *Caenorhabditis elegans* early development through 18S ribosomal RNA processing. Nucleic Acids Res. *32*, 1028–1036. https://doi.org/10.1093/nar/gkh264.

130. Zhu, C., Yan, Q., Weng, C., Hou, X., Mao, H., Liu, D., Feng, X., and Guang, S. (2018). Erroneous ribosomal RNAs promote the generation of antisense ribosomal siRNA. Proc. Natl. Acad. Sci. USA *115*, 10082–10087. https://doi.org/10.1073/pnas.1800974115.

131. Liao, S., Chen, X., Xu, T., Jin, Q., Xu, Z., Xu, D., Zhou, X., Zhu, C., Guang, S., and Feng, X. (2021). Antisense ribosomal siRNAs inhibit RNA polymerase I-directed transcription in *C. elegans*. Nucleic Acids Res. *49*, 9194–9210. https://doi.org/10.1093/nar/gkab662.

132. Updike, D.L., Hachey, S.J., Kreher, J., and Strome, S. (2011). P granules extend the nuclear pore complex environment in the *C. elegans* germ line. J. Cell Biol. *192*, 939–948. https://doi.org/10.1083/jcb.201010104.

133. Lev, I., Toker, I.A., Mor, Y., Nitzan, A., Weintraub, G., Antonova, O., Bhonkar, O., Ben Shushan, I., Seroussi, U., Claycomb, J.M., et al. (2019). Germ Granules Govern Small RNA Inheritance. Curr. Biol. *29*, 2880–2891.e4. https://doi.org/10.1016/j.cub.2019.07.054.

134. Dodson, A.E., and Kennedy, S. (2019). Germ Granules Coordinate RNA-Based Epigenetic Inheritance Pathways. Dev. Cell *50*, 704–715.e4. https://doi.org/10.1016/j.devcel.2019.07.025.

135. Ouyang, J.P.T., Folkmann, A., Bernard, L., Lee, C.Y., Seroussi, U., Charlesworth, A.G., Claycomb, J.M., and Seydoux, G. (2019). P Granules Protect RNA Interference Genes from Silencing by piRNAs. Dev. Cell *50*, 716–728.e6. https://doi.org/10.1016/j.devcel.2019.07.026.

136. Phillips, C.M., Brown, K.C., Montgomery, B.E., Ruvkun, G., and Montgomery, T.A. (2015). piRNAs and piRNA-Dependent siRNAs Protect Conserved and Essential *C. elegans* Genes from Misrouting into the RNAi Pathway. Dev. Cell *34*, 457–465. https://doi.org/10.1016/j.devcel.2015.07.009.

137. de Albuquerque, B.F.M., Placentino, M., and Ketting, R.F. (2015). Maternal piRNAs Are Essential for Germline Development following De Novo Establishment of Endo-siRNAs in *Caenorhabditis elegans*. Dev. Cell *34*, 448–456. https://doi.org/10.1016/j.devcel.2015.07.010.

138. Barucci, G., Cornes, E., Singh, M., Li, B., Ugolini, M., Samolygo, A., Didier, C., Dingli, F., Loew, D., Quarato, P., et al. (2020). Small-RNA-mediated transgenerational silencing of histone genes impairs fertility in piRNA mutants. Nat. Cell Biol. *22*, 235–245. https://doi.org/10.1038/s41556-020-0462-7.

139. Shukla, A., Perales, R., and Kennedy, S. (2021). piRNAs coordinate poly(UG) tailing to prevent aberrant and perpetual gene silencing. Curr. Biol. *31*, 4473–4485.e3. https://doi.org/10.1016/j.cub.2021.07.076.

140. Putnam, A., Thomas, L., and Seydoux, G. (2023). RNA granules: functional compartments or incidental condensates? Genes Dev. *37*, 354–376. https://doi.org/10.1101/gad.350518.123.

141. Thomas, L., Taleb Ismail, B.T., Askjaer, P., and Seydoux, G. (2023). Nucleoporin foci are stress-sensitive condensates dispensable for *C. elegans* nuclear pore assembly. EMBO J. *42*, e112987. https://doi.org/10.15252/embj.2022112987.

142. Kim, H., Ishidate, T., Ghanta, K.S., Seth, M., Conte, D., Shirayama, M., and Mello, C.C. (2014). A Co-CRISPR Strategy for Efficient Genome Editing in *Caenorhabditis elegans*. Genetics *197*, 1069–1080. https://doi.org/10.1534/genetics.114.166389.

Please cite this article in press as: Huang et al., Compartmentalized localization of perinuclear proteins within germ granules in *C. elegans*, Developmental Cell (2024), https://doi.org/10.1016/j.devcel.2024.12.016

STAR★METHODS

KEY RESOURCES TABLE

REAGENT or RESOURCE	SOURCE	IDENTIFIER
Bacterial and virus strains		
E. coli OP50	*Caenorhabditis* Genetics Center (CGC)	RRID:WB-STRAIN:OP50
E. coli Trans5α	Tsingke	Cat#TSC-C01
Chemicals, peptides, and recombinant proteins		
TS-GelRed	Tsingke	Cat#TSJ003
Proteinase K	BioFroxx	Cat#1124MG100
DpnI endonuclease	Thermo Scientific	Cat#ER1701
Critical commercial assays		
2x Rapid Taq Master Mix	Vazyme	Cat#P222-03
2x Phanta Flash	Vazyme	Cat#P520-03
ClonExpress MultiS One Step Cloning Kit	Vazyme	Cat#C113-02
TIANgel Midi Purification Kit	TIANGEN	Cat#DP209-02
AxyPrep Plasmid Miniprep Kit	Axygen	Cat#UE-MN-P-250
Deposited data		
Sequence file of transgenes	This study	Figshare: https://doi.org/10.6084/m9.figshare.26779972.v1; https://figshare.com/articles/online_resource/Plasmid_map_of_transgenes_constructed_by_mosSCI/26779972
Experimental models: Organisms/strains		
C. elegans	This study, Table S2	N/A
Oligonucleotides		
DNA oligos for genotyping insertions	This study, Table S4	N/A
*pid-2(ust628)*F: 5' AAGTCCCCGTGGAGTACA3'	This study	N/A
*pid-2(ust628)*R: 5' AAGTCCCCGTGGAGTACA3'	This study	N/A
Recombinant DNA		
pCFJ151	Addgene	RRID:Addgene_19330
pJK43.1	Addgene	RRID:Addgene_19332
pDD162	Addgene	RRID:Addgene_47549
pSG259	Author's laboratory	N/A
pSG280	Author's laboratory	N/A
Software and algorithms		
ImageJ 1.54f	https://fiji.sc/	RRID:SCR_002285
SnapGene 3.2.1	GSL Biotech LLC	RRID:SCR_015052
GraphPad Prism 9.0.0	GraphPad Software, Inc	RRID:SCR_002798
SensiCaspture	Peiqing Science & Technology Co., Ltd	N/A
Leica Application Suite X 3.7.4.23463	Leica	RRID:SCR_013673

EXPERIMENTAL MODEL AND STUDY PARTICIPANT DETAILS

Animal studies

C. elegans were grown at 20 °C for all experiments. Animals were maintained on nematode growth medium (NGM) plates seeded with *E. coli* OP50. The strains used in this study are listed in Table S2.

Please cite this article in press as: Huang et al., Compartmentalized localization of perinuclear proteins within germ granules in *C. elegans*, Developmental Cell (2024), https://doi.org/10.1016/j.devcel.2024.12.016

METHOD DETAILS

Construction of sgRNA plasmids and repair plasmids

Target sequences consisting of N20GG near the desired mutation sites were manually searched. The sgRNA sequences are listed in Table S3. To construct the sgRNA expression plasmids, the 20 bp *unc-119* sgRNA guide sequence in the pU6::unc-119 sgRNA(F + E) vector was replaced with the desired sgRNA target sequence via overlap extension PCR. The PCR products were directly transformed into Trans5α chemically competent cells.

For the construction of the repair plasmids, the 1.5 kb left and right homologous recombination repair arms of particular genes were PCR amplified for N2 animals; the vector was PCR amplified from pCFJ151; the coding regions of *gfp::3xflag, 3xflag::gfp*, *mCherry* or *tagRFP* fused to a linker sequence were PCR amplified from animals carrying these fragments. These fragments were joined together via Gibson assembly to form the repair plasmids using the ClonExpress MultiS One Step Cloning Kit (Vazyme Biotech, Nanjing).

CRISPR/Cas9-mediated gene deletion

Plasmids for injection were prepared using a miniprep plasmid purification kit (AxyPrep Plasmid Miniprep Kit, Axygen). The injection mixture consisted of 50 ng/μl Cas9-expressing vector(pDD162), 30 ng/μl sgRNA #1, 30 ng/μl sgRNA #2, 30 ng/μl sgRNA #3 and 5 ng/μl pSG259 vector. The mixture was injected into adult animals. After recovering from the injection, the worms were transferred onto OP50 plates (4 worms per plate). Three days after injection, F1 animals expressing pharyngeal GFP were isolated under a Leica M165 FC fluorescence stereomicroscope and transferred onto individual NGM plates to lay F2 animals for 4 days. F2 progeny from each plate were harvested with 50 μl of lysis buffer (500 μg/ml proteinase K) and screened via PCR amplification with the primers 5' -AAGTCCCCGTGGAGTACA-3' and 5'-TCGGTCAGCAGCAGCTTC-3'. Mutants with deletions were singled to NGM plates and further confirmed by PCR amplification and DNA sequencing.

CRISPR/Cas9-mediated gene tagging

The coding regions of *gfp::3xflag, 3xflag::gfp*, *mCherry* or *tagRFP* fused to a linker sequence, were inserted upstream of the stop codon or downstream of the start codon using the CRISPR/Cas9 system. We prioritized the use of *gfp::3xflag* and *3xflag::gfp* tags, as the *gfp* tag is the most frequently used label for imaging in nematodes and the *3xflag* tag is widely used for immunoprecipitation assays. For the insertion position (*3'* or *5'*), we prioritized selecting the positions reported in the literature. If we could not obtain the targeted nematode strains in two rounds of microinjection, in which at least 1,500 F1 animals with marker proteins were screened, we switched to another end for insertion. The injection mixture contained pDD162 (50 ng/μL), a repair plasmid (50 ng/μL), a marker plasmid (pSG259 (*myo-2p::gfp*::*unc-54_3'utr*) or pSG280 (*sqt-1p::sqt-1(e1350)::sqt-1_3'utr*) (5 ng/μL) and two or three gRNAs targeting sequences proximal to the N-termini or C-termini of the genes (30 ng/μL of each sgRNA plasmid,). The mixture was injected into adult animals. For knock-in lines in which pSG259(*myo-2p::gfp*) was used as the coinjection marker, F1 animals expressing pharyngeal GFP were isolated under a Leica M165 FC fluorescence stereomicroscope. For knock-in lines in which pSG280(*sqt-1p::sqt-1(e1350)*) was used as the coinjection marker, F1 rollers were isolated. Two strategies were then applied to identify targeted animals. (1) F1 animals were transferred onto individual NGM plates to lay F2 animals. The targeted animals with insertions were screened via PCR. (2) A strategy from an earlier study was adjusted and used.[142] 8-10 F1 adults were picked onto microscope slides, and the GFP fluorescence signals from germ cells were observed under a Leica DM4 B microscope. Worms with observable fluorescence in the germline were transferred from the slides onto individual NGM plates to lay F2 worms. Then, 16 F2 adults were singled onto individual NGM plates, and the homozygous transgenes were subsequently identified by evaluating fluorescence signals in F3 animals followed by PCR and agarose gel electrophoresis. The primer pairs used for genotyping are listed in Table S4. The CRISPR-modified DNA sequences were further verified via sanger sequencing and listed in Table S5. The sequence file of all ectopically expressed transgenes are stored in figshare (https://figshare.com/articles/online_resource/Plasmid_map_of_transgenes_constructed_by_mosSCI/26779972).

Quantification of brood size

L3 worms were individually placed onto fresh NGM plates. The numbers of progeny that reached the L2 or L3 stage were scored. n=10 animals.

Microscopy

To image larval stages, animals were immobilized in ddH2O with 0.5 M sodium azide and mounted on glass slides before imaging. To image embryos and germ cells in adult animals, worms were dissected in 2 μl of 0.4× M9 buffer with 0.1 M sodium azide on a coverslip and then mounted on freshly made 1.2%-1.4% agarose pads. The Leica THUNDER Imaging System was used, equipped with a K5 sCMOS microscope camera and an HC PL FLUOTAR 100x/1.40-0.70 oil objective, an HC PL FLUOTAR 20x/0.80 objective and an HC PL FLUOTAR 20x/0.80 objective. Images were taken and deconvoluted using Leica Application Suite X software (version 3.7.4.23463). The images in Figures 1D, 3J, 5, S2, S4C, S4H–S4K, S5A–S5E, and S6 were not deconvoluted. Images were rotated and cropped using Adobe Photoshop CS6 software. For the same proteins under different genetic backgrounds, equally normalized images were exported, and contrasts of images were equally adjusted between the control and experimental sets. As the expression levels of different perinuclear proteins vary, the display values of fluorescence images showing the relative position of perinuclear proteins within germ granules were manually adjusted to visualize these proteins using Leica Application Suite X software (version 3.7.4.23463). All images in this study are representative of more than three animals.

Please cite this article in press as: Huang et al., Compartmentalized localization of perinuclear proteins within germ granules in *C. elegans*, Developmental Cell (2024), https://doi.org/10.1016/j.devcel.2024.12.016

QUANTIFICATION AND STATISTICAL ANALYSIS

For the quantification of the relative fluorescence intensity of specific perinuclear proteins from the surface of the germline, individual germ cells at the pachytene stage were selected on the basis of the peripheral contour displayed via fluorescent signals, as reported in a previous study.[55] A total of 40 germ cells from 4 independent animals (10 germ cells per animal) were selected and the fluorescence intensity of each germ cell was analyzed by ImageJ.

For the quantification of the foci numbers of particular proteins in the rachis of the germline, 5 rachides from 5 independent animals were analyzed for each genotype. Three regions from the rachis of each germline were selected (14.6 × 14.6 μm^2 per region) and the number of foci in each region was counted. Each data point represents the total number of foci from the 3 selected regions from the same animal (3 × 14.6 × 14.6 = 640 μm^2).

The degree of colocalization between different fluorescently labeled proteins in germ cells was calculated using the Coloc2 plugin from ImageJ. Region of interest (ROI) masks covering individual germ cells at the pachytene stage were generated using the ROI Manager plugin. A total of 40 germ cells were selected from 4 independent animals (10 germ cells per animal). Coloc2 was used to generate a Pearson's R value for the degree of colocalization between two channels in the region defined by the ROI mask. Each data point represents the Pearson's R value, which represents the degree of colocalization between two fluorescence channels covering an individual germ cell.

To measure the fluorescence intensities across single germline nuclei in Figures 4B and 4G or a single germ granule in Figure 3I, lines in the merged images were drawn and the relative fluorescence intensities were analyzed using the "Line Profile" tool in Leica Application Suite X software (version 3.7.4.23463).

The mean values of the Pearson's correlation coefficient in Figures 2C, 3D, 3G, and S7A were calculated using GraphPad Prism software. Data in Figures 5, S1, and S6 are represented as mean ± SD. The significance values shown in Figures 5 and S6 were calculated with the Student's *t* test (two-tailed) via Excel. Sample sizes are indicated in method details.